Delft University of Technology

Faculty of Electrical Engineering, Mathematics & Computer Science
Department of Embedded and Networked Systems

Sensor Fusion for Localization of Autonomous Ground Drone in Indoor Environments

Gerardo Ivan Moyers Barrera

Sensor Fusion for Localization of Autonomous Ground Drone in Indoor Environments

Thesis

Submitted in partial fulfillment of the requirements for the

Master of Science

degree in

Embedded Systems

by

Gerardo Ivan Moyers Barrera

To be defended publicly on October 23 , 2020.

at

Delft University of Technology

Student number:	4820800	
Submission date:	October 18, 2020	
Thesis Committee:	Dr. Ranga Rao Venkatesha Prasad	Delft University of Technology
	Dr. Christoph Lofi	Delft University of Technology
	Dirk van den Heuvel	TOPIC Embedded Systems
	Dr. Vineet Gokhale	Delft University of Technology

Sensor Fusion for Localization of Autonomous Ground Drone in Indoor Environments

Abstract

Technology is transforming almost all aspects of our lives, one of them is automation. The main motivation of automation is to help humans avoid performing tedious, high risk jobs. Automated driving, also known as *autonomous driving*, has been at the center of industrial and academic attention since a few decades now, thanks to its potential of making driving risk-free by enabling a highly efficient machine control the vehicle on roads. Apart from the common outdoor use-cases, several applications in indoor environments have also been extensively investigated. The primary ones include process automation and management in large factories and warehouses.

Localization of the autonomous vehicle is crucial to determine the path to be followed to reach the desired destination. Sensor fusion techniques are extensively investigated for this. However, the major challenge arising in indoor environment localization is obtaining accuracy in the scale of a few centimeters in real-time. In this thesis, we intend to address this challenge. The contributions of this thesis are two-fold. Firstly, we develop a low-cost testbed – Autonomous Ground Drone (AGD) – that enables us to develop sensor fusion and localization scheme for autonomous driving. Secondly, we employ Extended Kalman Filter (EKF) on the sensor combination of UWB, IMU, and Radar, and achieve a localization accuracy of 8 cm. Our localization scheme outperforms state of the art in this field in terms of accuracy, latency, and power consumption.

Keywords: Localization, Sensor Fusion, EKF, AGD, low-cost, real-time

Acknowledgments

First, I will like to thank Dr. Ranga Rao Venkatesha Prasad and Dr. Vineet Gokhale for their support during the whole thesis. They provided a lot of suggestions and taught me how to perform research.

I would also like to express my sincere gratitude to Dirk van den Heuvel and Joris van Emden; they help me a lot during the whole design process and give me insides about the research. I learned so much about how to solve a problem and the phases of projects. A special thank you to my TOPIC colleagues, even though the COVID sent everybody home for a while, I enjoy the time spent together.

I would also like to take the opportunity to thank all the Mexidelftianos and LatiBoards2019 for their loving support during the master's. I am very happy to share many experiences with you and glad for all the things we learn and organize. These couple of years, you have become my family, and this couldn't be possible without them. Pablo Daniel Roberto Dacomba Torres and Hiram Rayo Torres Rodriguez, thank you for all the advice that you gave me during the thesis; you are a special part of my life, thank you for all the adventures we share. My dears BFFs, IDOLOs RP, Regina and Maggs thank you for keeping the friendship no matter the distance, during covid you were essential for my health.

This work will never be possible without the loving support of Estefania Trejo. Thank you for your companion and encouragement during the pandemic and the final phase of the thesis. Thank for all the adventures we have and all the laugh at random moments.Thank you to my brother Emilio Aron, your help me to keep pushing my self and support me during this master. Your advice and doubts during this process help me to discover new aspects that I haven't thought about.

Igual me gustaria agradecer a mi padre Emilio Gerardo, por todo su apoyo. Siempre nos has ayudado a cumplir nuestras metas y el terminar esta maestria fue mucho gracias a ti.Finalmente me gustaria agradecerle a mi madre Maria Guadalupe, tu apoyo incondicional cada día ha sido un "BOOST" para llegar a este punto. Gracias por como nos educaste a mi y a mi hermano, debido a eso estamos logrando nuestras metas.

Gerardo Ivan Moyers Barrera
Delft, The Netherlands
23 October, 2020

Contents

Chapter 1

Introduction

1.1 Autonomous Driving

Autonomous driving is the capability of a vehicle to perform maneuvers without any human intervention [33]. These maneuvers can be from cruise control to a complete drive. Besides user comfort, an autonomous vehicle has many advantages. The price of transportation and the CO_2 emission will reduce significantly [14] , road safety will increase [26], and industrial processes will be more efficient [16].

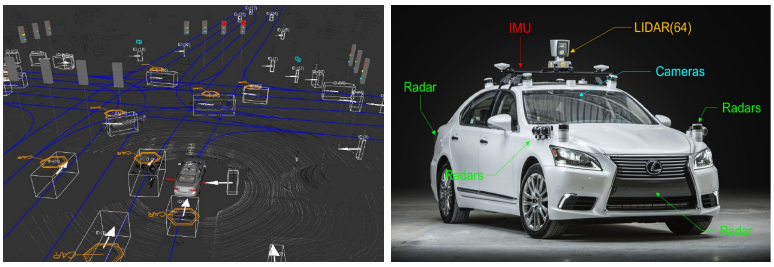

Figure. 1.1: Autonomous Driving Vehicle Example [26]

Autonomous driving has been studied since the 1980s, with the first incorporation being the Advanced Driver-Assistance Systems (ADAS) with the cruise control [14]. The automation has evolved, and the vehicles are capable of detecting objects on the road, like a vehicle, cyclist, pedestrians, walls, and react accordingly. A common scale used to measure the automation of a vehicle is the *SAE levels of automation* [42]. This scale goes from level 0 (no automation) to level 5 (full automation on all roads). Nowadays, few vehicles can drive in specific conditions (SAE level 3 [42]), making the task of driving easier and safer. However, there are several scenarios where these vehicles cannot function properly, e.g., tunnels, indoor environment, or GPS denied environments. Autonomous driving is not limited to cars, but also include other vehicles such as AGDs[16], Autonomous Unmanned Vehicles (UAV) [6] or trains [9], as shown in Figures 1.1 and 1.2 . Each vehicle will drive in different scenarios and with different actions to perform.

Figure. 1.2: Autonomous Driving Vehicle Example [44, 41]

Having a completely autonomous vehicle (SAE 4 or 5 [42]) will be beneficial to get the driving completed under any circumstances. Even experienced users are subjects to distractions while driving, resulting in fatal accidents accidents. Machines, on the other hand, will not get distracted, and crashes can be avoided. In industry, automating the driving process will benefit productivity. To achieve a fully autonomous driving, the vehicle should have these four main capabilities:

- Detection: The capability to sense the environment and know features, such as position, size, heading, and speed, of other objects on the road. These objects can be other vehicles, walls, signs, or pedestrians. Without detection, a vehicle will not be able to react to changes in the environment, increasing the probability of crashing.
- Localization: It is the ability of the vehicle to know its position and orientation on the road. Vehicles should not only be aware of the environment but also their localization to achieve a safe driving.
- Path Planning: The vehicles should be able to determine a path to follow in real-time in order, to reach the desired position. Just driving without a prior track will not only reduce the efficiency of the system as the power consumption but also makes autonomous driving an unsafe mode of transportation . This path is prone to change depending on the dynamic nature of the environment, such as sudden occurence of obstacles.
- Tracking: Predict and follow the trajectory of other vehicles or objects detected in the road. Even though the vehicle can sense the position of other objects, predicting their next action is desirable. The time the vehicle has to react is essential in autonomous driving. Tracking other objects in the road will increase this time and, in consequence, prevent accidents.

Most of the autonomous driving development is focused on vehicles in the outdoor environment. However, autonomous driving is not limited to these environments. Industries require automation of processes, and Autonomous Ground Drones (AGD) are used to drive in small places. In warehouses and factories, due to all the products stored, the space to drive is limited. Therefore AGD will need to drive through narrow paths. To be able to drive safely in those environments,

localization is essential. Performing faulty actions due to localization errors can produce critical failures. Even small errors in localization may result in crashes. Therefore, this thesis will focus on autonomous driving in indoor environments.

1.2 Localization in Autonomous Driving

Autonomous driving is a hot topic in industry and research; having a system that can efficiently detect the vehicle's self-position has been explored. In some scenarios, having small errors, even at a centimeter scale, will lead to system failures. If the Autonomous Ground Drone (AGD) has to drive through a narrow tunnel, few centimeters might be the difference between crashing or crossing the tunnel. Sensor fusion techniques have been explored to get the accuracy of the vehicles increased. The most common sensor used for localization is GPS; however, it has significant errors in indoor environment [43]. Therefore, Ultrawide Band (UWB) sensors are used for the same purpose [2]. Another widely used sensor is the Inertial Measurement Unit (IMU)[53], which delivers the heading and the acceleration of the system. Recently the integration of Light Detection and Ranging (LiDAR) sensors for localization has been explored. The vehicle can have a 360 field of view (FOV) and detect its position in the environment. Nevertheless, this sensor is expensive and delivers a considerable amount of data to process [38, 14, 43].

The task of localization in Autonomous Driving is crucial for achieving a safe driving. Localization is defined with three parameters position (P), orientation (θ), and speed (V). These parameters are sufficient to predict the trajectory of an autonomous vehicle. The vehicle needs information from its behavior, sensors supply this information. Several sensors are used to get the localization of the vehicles such as GPS, IMU, wheel encoder and LiDAR.

There are no perfect sensors; therefore, the localization may have errors in it. Errors in the localization will lead to faults on the system, from a small scratch to a fatal crash with objects. Besides these errors, some environments add a level of complexity to the task of localization, such as indoor environments. In an indoor environment, if an AGD is driving around, to get the exact position is crucial. Currently, the single sensors' accuracy is not enough. Therefore combining the data from different sensors has been studied [34, 16, 43]. Getting accurate localization will heavily benefit the autonomous driving task. Using several sensors instead of one increases the position's accuracy, makes the system more robust, gives the system the possibility of detecting objects, and reduces the chances of failure due to redundancy.

1.3 Sensor Fusion for Localization

Sensor fusion is the combination of data received from different sensors. Most sensors have the guaranteed performance only in certain situations, e.g., GPS will have good results on highways. However, if the vehicle enters a tunnel, then the measurements became unreliable. Therefore, fusing different types of sensors makes the system robust to different conditions [43]. The main objective of fuse

sensors in localization for autonomous driving is to increase the system's accuracy. Increasing this accuracy will benefit the whole task of driving. The vehicle will be able to drive through narrow spaces with a lower probability of collision towards the desired destination.

1.4 Challenges

This thesis will target indoor environments where the vehicle has limited space to drive, such as an office or a warehouse. Besides the narrow paths, density and NLOS are major challenges in indoor environments. Commons sensors like LiDAR and GPS will have poor accuracy. GPS has an unreliable performance in indoor environments. LiDAR needs a clear Line-of-Sight (LOS) to be able to calculate the localization. LiDAR is susceptible to hazardous weather and low lighting. In this thesis, we aim to perform accurate localization in an office-like environment. There will be several objects in the environment and narrow spaces where AGD has to drive through. As expected, this type of AGD will not have the processing capabilities as a top gamma vehicle, like Tesla 3. In this scenario, the project will have four main challenges:

1. High accuracy: Having an accurate localization of the vehicle is important for the system. Errors on the scale of a few centimeters might be the difference between crashing or driving safely in the office. In an office, there will be different objects. From the vehicle's perspective, this will mean that there will be objects behind other objects. A system with the capabilities of getting its self-position at GPS denied environments and with NLOS scenarios will be helpful. Increasing the accuracy of the whole system is one of the most important goals of this thesis.

2. Low-cost: Keeping the low-budget scalability in mind, it is crucial to select low-cost sensors with high localization accuracy. Additionally, since the environment is an office, sensors capable of detecting other objects will benefit the system.

3. Real-time localization: Autonomous driving is a task that depends extensively on the real-timeliness of the different steps involved (explained earlier). Hence, a system capable of performing the localization with a latency of a few milliseconds is desired. The AGD performs the complete localization on the move, so real-time localization is essential.

4. Energy-efficiency: In autonomous driving, the processor's operation frequency and memory space are relevant aspects to consider. This will limit the amount of data that can be processed efficiently in a period, as the method to process the data. Also, selecting the right sensors is also crucial for energy-efficiency.

1.5 Research Statement and Contributions

The problems focused on this thesis will be to achieve a better performance than the state of the art for localization and reducing the cost of the system. Most of

the research is implemented in a controlled environment making it unfeasible to deploy it in real scenarios. Therefore one of the goals is to test this system in a real environment.

The challenges for *localization in indoor environments* focused in this thesis will be addressed in a novel *sensor fusion* implementation. The design will be made by choosing low-cost sensors and performing an energy-efficient algorithm maximizing fusion accuracy. The design process involves a fusion of IMU, UWB, and 3D Radar. To the best of our knowledge, this is the first attempt in exploring the fusion of these three sensors on an AGD for localization. State of the art in localization at indoor environments fuse IMU, LiDAR, and UWB, and it has a Root Mean Square Error (RMSE) of 10 cm. This work aims to get higher accuracy with the sensors' fusion and reduce the cost, computation, and power consumption of the whole system. Also, evaluate the performance of the Extended Kalman Filter (EKF). To consider the project successful; i), the system must perform a safe drive. ii) Fusion of the three sensors give relevant results. iii) Fusion can work in different environments

The research questions of this thesis are the following:

1. Which fusion of sensors will deliver the best result in localization?
2. What will be the trade-off between cost and performance for the system?
3. Is it possible to obtain better energy performance of the vehicle?

In localization sensors as IMU, UWB, GPS and Lidar are the most commonly used. Applying a fusion of these sensors improves the accuracy of the system [17]. In this thesis, a fusion between UWB, IMU, and Radar for an AGD is explored as shown in Figure 1.3. The main contributions of this thesis are as follows:

- We develop a low-cost AGD with on-board UWB, IMU, and Radar for localization in indoor environments.
- We develop sensor fusion of the above sensors using EKF. The weights for each of these sensors are chosen carefully via extensive experimentation.
- We propose an adaptive localization strategy depending on the sensor signals. The primary parameters of interest in this thesis are location accuracy, energy consumption, and localization latency. It is carried out extensive performance evaluation of localization using our strategy using our testbed. Our results show an accuracy of 8.54 cm, energy performance of 3.95 W, and latency of 2.66 ms.

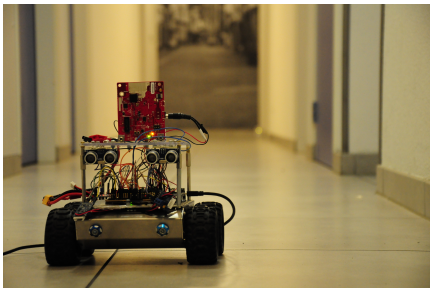

Figure. 1.3: AGD final.

This thesis was developed in collaboration with the company TOPIC embedded systems. TOPIC provides the hardware and physical space to develop the project. Particular interest has been increased in the automotive sector due to the advances made in autonomous vehicles. The organization wants to contribute to the evolution of this technology by designing automated unmanned vehicles.

1.6 Thesis Outline

This work is structured as follows. Chapter 2 will discuss the state of the art of sensor fusion, autonomous driving, and localization in indoor environments and give insight into this thesis's motivation. The testbed design and its requirements will be explained in Chapter 3. Chapter 4 presents the steps made during the implementation of the fusion algorithm. The description of the test environments, testing, and results will be given in Chapter 5. Finally, conclusions and future work are exposed in Chapter 6.

Chapter 2

Related Work

An ever-increasing number of vehicles has been the root cause of several problems such as traffic congestion and road accidents. In the past decade, there has been a growing interest in autonomous driving; therefore, a lot of research had been carried out. Autonomous driving is a challenging domain as it involves several complex problems such as a phase of detection, a phase of planning, and a phase of execution. Accurate sensor data acquisition followed by their fusion is crucial for achieving safe and efficient maneuvering; errors in centimeters' scale could lead to crashes.

2.1 State of the art

Different sensors can be used to get a more reliable system; these sensors can be Radar, LiDAR, Global Navigation Satellite System (GNSS), Real-Time Kinematic (RTK), Global Positioning System (GPS), IMU (accelerometer and gyroscope), or stereo camera. Due to limitations on a single sensor's accuracy [43], topics like Simultaneous Localization And Mapping (SLAM) and sensor fusion have been the focus of extensive research. Therefore sensor fusion schemes have been investigated for indoor environments to enable small robots and vehicles to drive autonomously in any scenario.

2.1.1 Sensor Fusion

Sensor fusion is a technique that combines the information acquired from different sensors for obtaining higher accuracy. These sensors can be homogeneous or heterogeneous. In a homogeneous case, few sensors belonging to the same type are deployed in different locations, whereas in heterogeneous cases, different types of sensors are deployed in the same location to improve the diversity in signal acquisition. Sensor fusion can be divided into three main categories; Low-level fusion (raw data), middle-level fusion (specific features of the data), and high-level fusion (track data) [26]. There is also a possibility to apply fusion at different levels simultaneously; this is called hybrid fusion [22]. Sensor fusion has a wide scope for autonomous driving; most research is focused on the following topics:

- Localization: The most common sensors are LiDAR, camera, GPS, and Radar [43].
- Path planning: The use of Radar, cameras are common in path planning; nevertheless, sensors like IMUs, wheel encoders, GPS, LiDAR are also used [32, 41].
- Tracking: The sensors used for motion tracking are IMUs, wheel encoders, GPS, Radar; however, if the tracking is from a different object, then LiDAR and cameras are useful [40].
- Object detection: It is extremely desired to get have vision sensors for object detection; therefore, sensors like LiDAR, camera, and Radar are often used. The high-level fusion is commonly applied for object detection; neural networks (NN) can be an example [14].

Sensor fusion can be broadly divided into two categories: (i) Heuristic - is easy to implement; it uses experimental data and fuses the ones with more similarities [27], e.g., in object detection, heuristic fusion will combine the objects with the smaller distance between them. In localization, the heuristic fusion will compute the average of the positions delivered by all the sensors., (ii) track-to-track it is a fusion based on the estimates of position; Mahalanobis distance and the covariance help get the probability of estimation and take that into account in the fusion. Experiments like [27] indicates that track to track fusion achieves better results. In literature there are different methods that use track-to-track fusion, these can be separated in filter-based and optimization-based [28, 17]. Track to track will take features of the sensors and fuse them to achieve a more accurate estimation. In the rest of this thesis, the focus will be only on track-to-track fusion.

Filter-Based

As the name suggests, filter-based methods perform filtering on the data to calculate the position of the vehicle, mostly in an iterative fashion [17]. This filtering majorly serves to reduce the impact of noisy measurements and therefore increases the accuracy. Different filter-based algorithms are described below:

- Kalman Filter (KF): It is a recursive data processing algorithm used for the estimation of states of a system from noisy measurements [32]. KF consists of a recursive algorithm with two main steps: prediction and update. The prediction step uses past estimation to calculate the next position of the vehicle. The update step compares the prediction with the measurements and updates the position. This technique has been used extensively for autonomous driving. There are some variants like Extended Kalman Filter (EKF) [54], Unscented Kalman Filter (UKF) [17], Federated Kalman Filter (FKF) [54], Adaptive Kalman Filter (AKF) [29] that are used in practise.
- Particle Filter (PF): This is a type of Bayesian Filter (BF) state estimation approach that calculates the probability of multiple predictions so the user can infer its actual position [24]. This is a sampling-based technique used for nonlinear measurements or multi-rate processing scenarios [40, 25]. PF is

analogous to spreading particles through the environment with equal probability, and after a movement of the vehicle, eliminate the ones with less probability [40].

- Histogram Filter: This is a nonparametric method that approximates the posteriors by decomposing the state space into finitely many regions and representing the cumulative posterior for each region by a single probability value [18].
- Gaussian Mixture Probability Hypothesis Density (GM-PHD): A GM-PHD filter uses multi-object tracking implementations. This is handled with a measurement-to-track association that is based on Random Finite Sets models [31].

Optimization-Based

These techniques rely on two steps, training and prediction [17]. During training, the algorithm uses data previously recorded from the sensors and identifies constraints. During prediction, the position is calculated based on the constraints. Different optimization-based algorithms are described below:

- Permutation Matrix Track Association (PMTA): This is a novel track association algorithm for multi-sensor fusion scenarios, considering spatial and temporal information. The advantage of PMTA is that it reduces the ambiguity of track association between multiple sensors by constraining the different tracks to one by one [26].
- Information Matrix Fusion (IMF): This is based on using the information form of the error covariance. IMF is obtained by taking the inverse of the error covariance matrix [29]. This technique is used to track temporal correlation [26].
- Graph optimization: This is a technique often used for SLAM applications due to its ability to allow for delayed incorporation of asynchronous measurements [37].
- Deep learning: Since machine learning has become popular in the recent years, convolutional NN (CNN) has also been explored in the area of sensor fusion and has been found to be extremely reliable [14]. Deep learning is used to compute algorithms that have to be trained by a huge amount of data. Programs that can work with NN are suited for these applications, like Tensorflow [52].
- Covariance Intersection (CI): A fusion technique that involves weights to fuse two Gaussian estimates [26].
- Bundle Adjustment: This is a technique that optimizes the fusion of 3D with 2D measurements. Most of the applications are focused on SLAM [17]. The most common algorithm for bundle adjustment is using the Levenberg Marquardt [17].

2.1.2 Indoor Environments

Autonomous driving faces many challenges; one of them is to work in indoor environments effectively. GPS is a widely used sensor; unfortunately, when there is no direct Line Of Sight (LOS), it gets extremely noisy. Wireless IPS has become popular in recent years to replace GPS. IPS uses mostly short-range radio, such as WiFi, RFID, ZigBee, or ultrasound [2]. Most of the research made in IPS uses the Received Signal Strength (RSS) and the Angle of Arrival (AOA) parameters to determine a position [57]. Even though WiFi infrastructure is already installed in most buildings, the accuracy is not enough to consider for autonomous driving [3]. The applications for IPS may vary between localization, object detection, and tracking. Different sensors can be useful; these sensors can be divided into two main categories [1]:

Passive Sensors

A passive sensor is the one that does not require an interaction (response) from the environment. This type of sensors will define a position based on the observability. Different types of passive sensors are listed below:

- Optical: The detection of these sensors relies on visibility. Because computer vision has been a hot topic for research in the past decades, implementations with optical sensors already exist. A downside is that they require a LOS of the object to detect it [1], hidden objects at some time step may cause a fatal accident. The most common optical sensors are cameras. These sensors also have a decrease in their performance in bad weather with poor illumination.
- Infrared: Like an optical sensor, it requires a LOS for detecting an object; an advantage of an infrared sensor is that it is less dependent on visible light. Infrared sensors can distinguish between human beings and objects because it can distinguish objects based on their temperatures [1].
- Acoustic: A common acoustic sensor is a microphone. This will detect an object by using the time distance of arrival algorithms [1]. A big problem for these sensors is that they are extremely susceptible to noise.
- Inertial Measurement Unit (IMU): It is a combination of accelerometer, gyroscope, and magnetometer. It measures the linear acceleration and angular velocity of a vehicle and, with these values, obtains the position, velocity, and orientation. It is important to notice that IMU senses the behavior of the AGD and not objects in the environment.

Active Sensors

In contrast with passive sensors, active sensors require a transmitter and a receiver for sensing the environment. This means that the system is extremely prone to interference when multiple transmitters are present in the neighborhood. Different types of active sensors are listed below.

- LiDAR: LiDAR works by transmitting a light pulse and detecting the reflection to determine the distance to the object. By doing this detection at

different angles, LiDAR can obtain an accurate estimation of the environment. As with cameras, when an object is present with No Line Of Sight (NLOS), it is impossible to detect it [1].

- RFID: These sensors use tags to identify their detection. The RFID is very useful for tracking applications; the disadvantage is that it requires an infrastructure in place [1]. These sensors are commonly used in indoor environments, UWB one of the most accurate [55]. A big advantage is that it is not required to have a LOS to obtain accurate results [1]; nevertheless, it results in a slight reduction in accuracy.

- Radar: It works by transmitting radio waves to the environment and measure the reflections. A huge advantage of this sensor is the detection of the object, even with NLOS. The Frequency Modulation Continuous Wave (FMCW) based radars deliver relative distances and speed of objects [5].

2.1.3 Sensor Fusion for Localization

The fusion methods explained in this chapter can be applied to autonomous driving like object detection, localization, path planning, and tracking. However, for localization, the most common methods are the filter-based [43]. IMU, LiDAR, RFID and Radars sensors are the one that delivers relevant data for localization of the vehicle [15, 23]. In literature, variants of the KF are widely used; EKF being the most used as in [9, 5, 51, 4], these research use different sensors like Radar, GPS, LiDAR, and IMU to reach centimeter accuracy in indoor and outdoor environments. In [18] an Error State KF is used to fuse a LiDAR, IMU, and GPS aiming for an accuracy of several centimeters in outdoor environments.

Besides KF, PF has shown promising results in sensor fusion for localization, [40] uses PF and compared performance with UKF fusing a magnetometer with an accelerometer. PF is also used in [15], here the focus is a network of vehicles incorporating communication between vehicles, as a new measurement, to calculate the localization. A GM-PHD filter is used to fuse LiDAR with a stereo camera, capable of computing the depth, IMU and GPS capable of localizing at 20 km/hr in outdoor environments [31].

Indoor environments are challenging due to their inability to use GPS. An effort has been made to find a sensor similar to GPS that works in indoor environments. The most promising sensor is the UWB [35]; nevertheless, there are some attempts to fuse it with different sensors [55] where LiDAR and UWB are fused using EKF. Other attempts to fuse UWB is explained in [2], where IMU is combined with the UWB. The disadvantage of UWB is the requirement of infrastructure setup. Attempts like [56] avoid the use of UWB and infrastructure set up by fusing Radar and ultrasound.

LiDAR is a promising sensor to achieve accurate localization; extensive studies have used this sensor [55, 38, 53]. However, LiDAR is an expensive sensor, drains a considerable amount of energy, and generates a huge amount of data, e.g., Hokuyo UTM-30LX-EW used in [55, 53]. Indoor localization research typically focuses just

on the accuracy of the system, ignoring important data like latency to achieve a real-time computation [2, 56].

Chapter 3

Testbed Design

In this thesis, a localization method is explored to increase the accuracy of the localization of an autonomous vehicle in indoor environments. This fusion aims to perform efficiently in real live scenarios; therefore, it is needed an AGD with all the sensors. The most effective way to develop a fusion technique and evaluate its performance is by building an AGD testbed. In this chapter, we describe the design details of the AGD testbed that we developed towards fulfiling the objectives of this thesis. To evaluate the testbed, a real-life AGD is required.

3.1 Requirements

The thesis's first challenge was to make an AGD capable of driving to pre-defined locations in indoor environments. Furthermore, the vehicle should be able to localize itself in different environments, long corridor, and an office, as can be seen in Figures 3.1a and 3.1b. The design will follow recent researches focused on localization at indoor environments [56, 55, 53, 2]. The general requirements for the testbed are as follows:

1. High-accuracy: The AGD should drive around narrow paths; a localization error of maximum 30 cm is necessary [43, 17].
2. Real-time performance: The task of autonomous driving requires real-time processing; therefore, special consideration has to be in the sensor's sampling rate, typically bigger than 5 Hz [17, 18, 37].
3. Latency: Keeping in mind the real-time requirement, special attention was invested in the computation time. Using sensors which do not deliver a huge a mount of data will collaborate on minimizing the latency.
4. Energy-efficient: Since the AGD powered by batteries, a focus on the power consumed by each sensor is required. Sensors with an average consumption bigger than 5 W are not going to be considered. Data load is an important parameter to reduce power consumption. Therefore, sensors that deliver a huge amount of data are not desired.

5. Dimension: The AGD is small, as described in Chapter 1; therefore, there is a constraint on the sensors' dimensions. The sensors will be placed near to each other. The dimensions of the vehicle can not exceed 30 cm width and long and 50 cm tall. Besides the dimension of the AGD, by placing the sensor near each other, it avoids the conversion of the data to the gravity center of the vehicle.

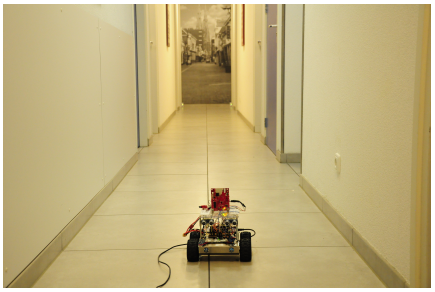

(a) Long corridor environment.

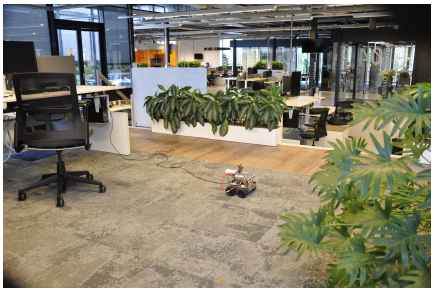

(b) Office environment.

Figure. 3.1: Showing the two different test environments used in this thesis for testing our localization method.

3.2 Architecture

3.2.1 Hardware

Selecting which sensor will be more suitable for the system is an important task. As mentioned in the previous chapter, the AGD should localize itself, have real-time processing, low-power, designed with a low budget, and detect objects. Due to localization being the main objective of this thesis, all sensors should deliver relevant data for this objective. Due to the vast amount of data to process and no energy-efficient, sensors such as; cameras and LiDAR are out of the scope.
Finally, besides Radar and UWB will be able to localize the vehicle, but they do not give any information about the orientation. For determining the orientation of the AGD, we will use an IMU onboard the vehicle.

The hardware architecture of the testbed is shown in Figure 3.2. Besides the sensors and the processor, motors and power supply are considered in the design. A description of the modules is described below:

- DC motor: 5 V motors with an H-bridge to control the speed and direction.
- Power supply: Lipo 2S battery of 3000 mAh so the system can run for several hours straight. Since the board and the sensors have to be powered by 5 V, a DC-DC converter is used.
- Radar: Radar is a perfect match for serving the project objectives since; they can detect objects and localize the self-position with no huge amount of data

and errors smaller than 30 cm. The power consumption of this sensor can be smaller than 5 W. Radar is not an expensive sensor, so it fulfills the testbed requirements. The communication with the board is via UART.

- UWB: At this moment, the best sensor to get self-localization in indoor environments is the UWB; therefore, integrating it into the AGD will benefit the system. The energy, volume of data, and cost of this sensor are low. The data will be transmitted via UART to the board
- IMU: For determining the orientation of the AGD, we will use an IMU on-board the vehicle. It is a common sensor used in localization, giving accurate results. The price of this sensor is usually a few euros. The data load and power consumption of IMU are minimum. The communication protocol with the board will be I^2C.
- Ultrasound (US): An ultrasound will be used as a *safety* sensor to avoid collisions; this sensor immediately brake the vehicle if it detects an object in front within a distance of 15 cms.

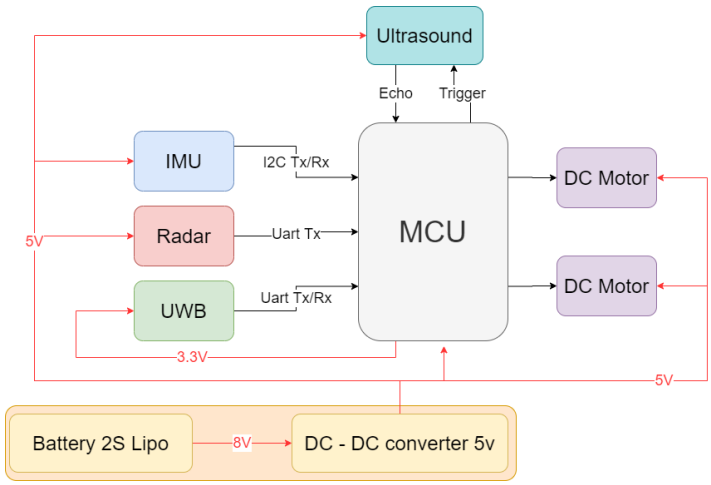

Figure. 3.2: Hardware Architecture of our testbed.

3.2.2 Software

Combining the data acquired from a multitude of sensors is not a trivial task. Fusion methods are often used; filter-based and optimization-based methods [17] have been proved to have good results [37, 51]. Nevertheless, optimization-based requires a large amount of memory. The system has a limitation in this area, so for this work, the filter-based methods are going to be implemented. Kalman filters are widely used to achieve fusion for localization [2]. As described in Chapter 2, KF is used for the estimation of states. Due to the non-linearity of the sensors, a simple KF will not deliver accurate results. Nevertheless, some variations like EKF make compensation for the non-linearities of the system. The EKF will predict the position of the vehicle based on the measurements of the sensors. The software architecture is shown in Figure 3.3; all the computation will be performed in the

microcontroller. Three main modules are described as follows:

- Data processing: The data from the sensors have to be computed to obtain the values of position, speed, and orientation. Each sensor will require different computations, as it will be explained in Section 3.3.
- EKF fusion: The EKF will receive values of position, speed, and orientation from the Radar, UWB, and IMU. These values will be used to estimate the localization of the AGD.
- Motor Control: To control the vehicle's speed and orientation, data from the IMU is used. A PID controller will process this data.

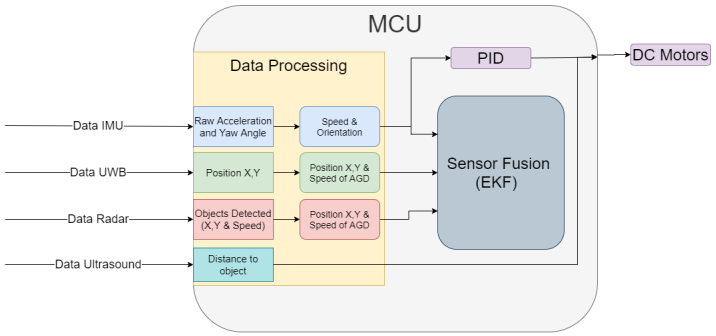

Figure. 3.3: Software Architecture of our testbed.

3.3 Implementation

For this thesis, the testbed will be implemented using a microprocessor STM32L4R5ZI incorporated in a NUCLEO-L4R5ZI microcontroller board [45]. As was mention in Chapter 2 the vehicle will have a Radar, IMU, and UWB for localization and an ultrasound for emergency braking . The board and sensors used are listed below:

1. Microcontroller: NUCLEO-L4R5ZI [45]
2. Radar: AWR1843 [50]
3. IMU: MPU6050 [21]
4. UWB: DWM1001dev [11]
5. Ultrasound: HC-SR04 [13]

In the following section, we will describe the sensors' specifications and configurations for the localization in detail.

3.3.1 Processor

The NUCLEO-L4R5ZI is a developer board with an ARM Cortex M4 32 bit microcontroller with an operating frequency of 120 MHz. It also contains high-speed memories (flash memory up to 2 MB, up to 640 kB of SRAM). A key feature for choosing this board was the available options for communication; the NUCLEO has 6 USARTs, 4 I^2C, and 3 SPI [47]. The communication used in this thesis is via USART 2 for connecting the UWB, USART 3 for the Radar, and I^2C 1 for the IMU. The UWB communication requires Tx and Rx channels. In the case of the Radar, only an Rx channel is used. The I^2C requires two different I/O, a synchronization clock (SCL), and a data line (SDA). All of these registers are on the set of headers CN11 and CN12 [45]. To be able to use it, some soldering has to be done; in Figure 3.4 can be seen the connections to the board. The board was selected, taking into account the number of communication pins, the operating frequency, and memory. In comparison to Arduino Mega [30] or with Nucle L476RG [46], this board has a higher operating frequency, enough communication pins for all the sensors, and larger memory.

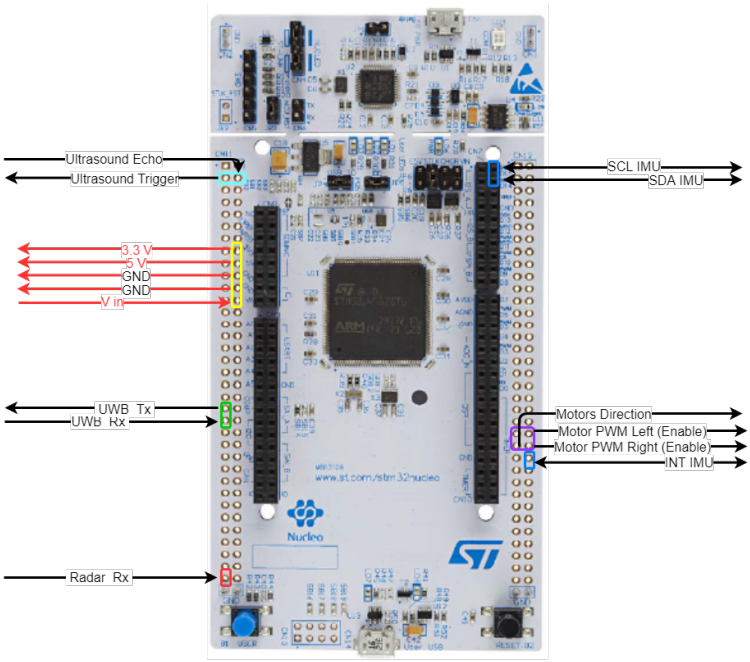

Figure. 3.4: Diagram of connection fron NUCLEO-L4R5ZI board to Radar, UWB and IMU [45]

3.3.2 Radar

Keeping the project objective mentioned earlier in mind, the following are the desired capabilities of a Radar: Being able to transmit via *UART* or I^2C, range detection of about than 40 meters, and resolution of 10 centimeters or less, and be

able to the detect at which height is the object detected. The mmwave *AWR1XXX* [48] radars from TI fulfill most of the requirements; however, the only capable of 3D detection is the *AWR1843BOOST*. The AWR1843BOOST has 4 Rx and 3 Tx antennas, as shown in Figure 3.5, so that it can have 3D detection of the environment [50]. FMCWs radar can be configured for medium or short range. Typically medium range is from 40 m to 150 m with a resolution of 70 cm, able to detect an object moving at 150 kmph with a field of view (FOV) of $\pm 15^{\circ}$ [7, 50, 48]. Medium range detection is often used for path planning, collision avoidance, and tracking other object highways. On the other hand, short-range is used to have accurate detection of objects. This configuration has a maximum range of 40 m with a minimum resolution of 4 cm, a maximum speed range of 36 kmph, and a FOV up to $\pm 100^{\circ}$ [7, 50, 48].

Typically in a warehouse setting, there could be several objects in the vicinity of the vehicle. Hence we chose the short-range configuration. The Radar's factory settings are a range of 150 m with a resolution of 35 cm; setting all the parameters to obtain the desired values was a challenging task. The *AWR1843BOOST* is a relatively new sensor, so there is not much documentation on how to change the parameters as in other mmwave radars. To modify the resolution, the values of start frequency (f_c), bandwidth (B), and duration (T_c) have to be changed. With these values, it can be calculated the slope (S) of the signal [49]. Using the Equation (3.1) where c is the speed of light, and Δd is the resolution can be set to $4.3\,\mathrm{cm}$ using the following values:

- T_c= 87 μS
- f_c = 77.1 GHz
- B = 3.66 GHz

$$\Delta d = \frac{c}{2ST_c} \tag{3.1}$$

Using this configuration, the maximum range is 20 m. To transmit data from the AWR1843BOOST to the NUCLEO-L4R5ZI, two more changes have to be made. The first is that the UART pin on the Radar is disconnected; therefore, a 0 Ω resistor has to be soldered in position R26. The second change is to decrease the Radar's baud rate from 921,600 to 204,800 Hz so it can use the maximum baudrate of the microcontroller. The configuration of all the Radar parameters has to be performed in three steps to be uploaded to the AWR1843BOOST.

1. Modify and build a program with new configuration parameters.
2. Turn switch 0 and 2 ON and switch 1 OFF, of jumper S1, to flash the AWR1843BOOST with the pre-built binaries from step 1.
3. Turn switch 2 OFF, of jumper S1, to enter into the running mode to start detecting the environment.

The Radar will deliver the message that will contain the number of objects detected, their position in X, Y, and Z coordinates and the relative speed of the

object. By giving an initial position, the Radar can track its movement by averaging the movement of the objects detected. Obtaining the position of the vehicle was quite challenging. The algorithm designed involves a previous knowledge of the vehicle's position, and the Radar will measure the displacement of it. The displacement was calculated by averaging each object's displacement detected comparing a previous measurement with the actual. Following a similar approach described in [17, 43, 37], it can be calculated the distance that the vehicle moves with Equation (3.2), where P is the position of the object k, N_{obj} is the total number of objects detected by the Radar. In this case, all the objects with a relative speed different from the vehicle will be discarded.

$$d = \frac{\sum_{n=1}^{N_{obj}} P_k - P_{k-1}}{N_{obj}} \tag{3.2}$$

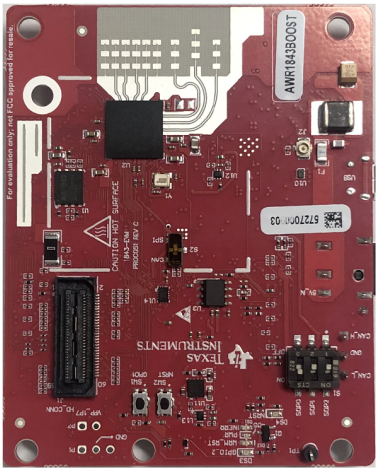

Figure. 3.5: AWR1843BOOST EVM front view

3.3.3 IMU

The IMUs are widespread sensors used in many industrial applications. Therefore, there are different chips, in the market, with capabilities similar to each other. Rather than the general requirements, the IMU has to should have the following desired capabilities: have a scale bigger than 4g and 500 dps for the accelerometer and the gyroscope, respectively, have $UART$ or I^2C communication protocol. The MPU6050 is formed by an accelerometer and a gyroscope giving a detection of 6 axes of motion to the chip. The sensor will be placed in the middle of the vehicle having the x-axis positive to the front, y-axis positive to the right, and the z-axis positive to the bottom. The gyroscope and the accelerometer have different ranges of operation, as described in [21]. Due to the high accuracy needed, we chose the highest possible resolution of 2000 $^\circ/s$ (dps) for the gyroscope and $\pm$ 16 g for the accelerometer. The MPU6050 has a maximum output rate of 1 kHz. To send the data to the Nucleo board, it uses the I^2C communication protocol. The raw data from the MPU6050 cannot be used directly, so some calculations have to

be performed. Following the sensitivity table on [21], the accelerometer raw data has to be divided by 2048 to scale it to 1 G, where G denotes the gravity of the earth. For the gyroscope raw data, it has to be divided by 939.650784 to scale it to radians per second.

Once the data is converted to the desired units, it was taken ten samples of the IMU and calculate the mean to get a better accuracy of the measurements. The accelerometer measurements are susceptible to noise; therefore, a combination of accelerometer and gyroscope was applied to make the measurement more robust to noise. The first step of this combination is to convert the gyro data into the same units as the accelerometer with Equations (3.3) and (3.4) [20]. Let R_x and R_y the values converted, r_x and r_y are the roll and pitch angles at each time step of the vehicle.

$$R_x = \frac{sin(r_y)}{\sqrt{1 + cos(r_y)^2 * tan(r_x)^2}} \tag{3.3}$$

$$R_y = \frac{sin(r_x)}{\sqrt{1 + cos(r_x)^2 * tan(r_y)^2}} \tag{3.4}$$

To combine the converted data with the data from the accelerometer it was used Equation (3.5) [20], where w_G is how much it is trusted the values of the gyroscope, R_A is the data from the accelerometer and R_G are the and the converted values from the gyroscope. R_A, R_G and R are vectors with x,y,z coordinates.

$$R = \frac{R_A + R_G * w_G}{1 + w_G} \tag{3.5}$$

These values are used to control the movement of the vehicle with a PID controller. A diagram of the PID controller is shown in Figure 3.6 where K_p, K_i and K_d are 4, $4 * 10^{-4}$ and 0.115 respectively. The input of the PID controller will be the angle and the acceleration of the vehicle. Besides controlling the vehicle, the IMU data will estimate the vehicle's position in the fusion algorithm.

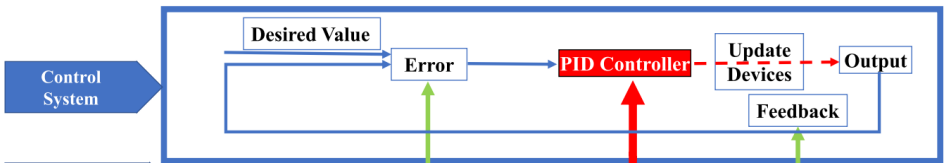

Figure. 3.6: Block diagram of PID controller used in our testbed [19].

3.3.4 UWB

This UWB was selected because it has an accuracy of 18 cm and a sampling rate of 10 Hz, which is favorable for meeting the project objectives. The Decawave DWM1001dev can be configured into three modes: anchor, tag, and listener [10]. The anchor is at a fixed position and transmits a message noting the transmission time and wait for the broadcast from the tag to determine the distance between

both. The tag will wait for the message from the anchor, and with the reception time, calculate the distance to the anchor at the same time transmit a broadcast message to all the anchor nearby. The listener works only to transmit data to other boards; this will contain the position of all the tags in the network. The DWM1001dev works with a Two Way Ranging (TWR) algorithm to determine the position of the tags [12]. As can be seen in the Equation (3.6) [35], the distance between the anchor and the tag can be easily calculated, where t_1, t_2 the time of reception of the tag and anchor respectively. Nevertheless, this distance is only in 1D. By knowing the anchors' position and its distance to the tag, we can calculate the 3D position of it with a trilateration [35] as it can be seen in Figure 3.7. The circles made with the trilateration will have a distance between the tag and the anchor, being the center's anchor. The position of the tag will be where the four circles converge.

$$d = c * \frac{t_2 - t_1 - t_{reply}}{2} \tag{3.6}$$

To make this UWB work efficiently, it is necessary to place at least four anchors throughout the environment. By setting the four anchors at different positions, the system can get a 3D position of the tag in X, Y, and Z coordinates. The different working rates of the DWM1001dev are from 1 to 10 Hz; in this thesis, it is chosen the maximum frequency. A tag will be placed on top of the vehicle to track its position over time. The tag and the anchor can only communicate with the UWBs on the network; therefore, to get the vehicle's position transmitted to the board, it is needed a listener. The listener is connected via UART to the board with a baud rate of 115200. The vehicle's speed was computed using Equation (3.7), where U the position measured by the UWB; this was multiplied by a factor of 10 to convert it into m/s units.

$$V = (U_k - U_{k-1}) * 10 \tag{3.7}$$

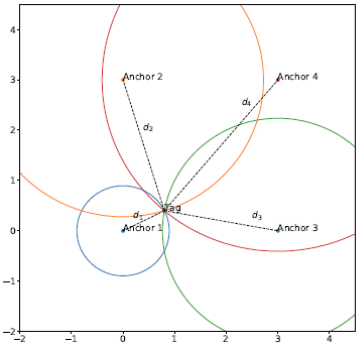

Figure. 3.7: TWR trilateration [35]

3.4 AGD dimensions and cost

The AGD dimensions are 20 cm length, 14 cm width and 27 cm tall. The sensors' position was selected to be as near as possible to the center of the vehicle, as mentioned previously in this chapter. In Figure 3.8 is shown the shell of the AGD with out the sensor incorporated. The shell has a weight , also considering the wheels and motors, of 1.3 kg.

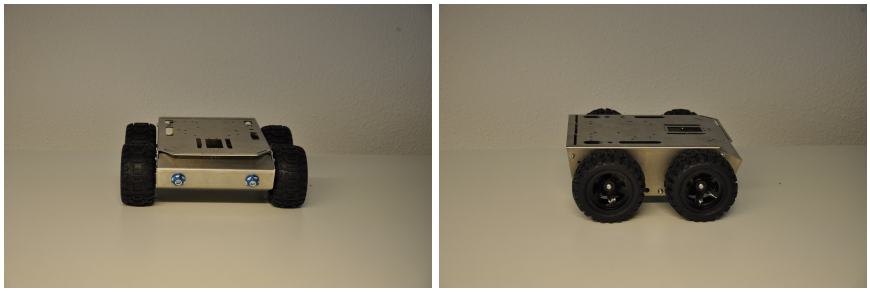

Figure. 3.8: Hind and side views of the shell for the testbed.

The Radar will be at the center and the highest level of the vehicle to reduce the impact of faulty detections on the floor. The UWBs onboard are two, a listener and a tag, the tag to track the localization of the AGD and the listener to transmit this data to the microcontroller. The tag was placed behind the radar on the top level. The IMU will be placed on the base of the vehicle near the center. The ultrasound, as a safety sensor, will be placed at the front of the vehicle. In Figure 3.9, the AGD built during this thesis is shown. The cost of the whole vehicle is described in Table 3.1.

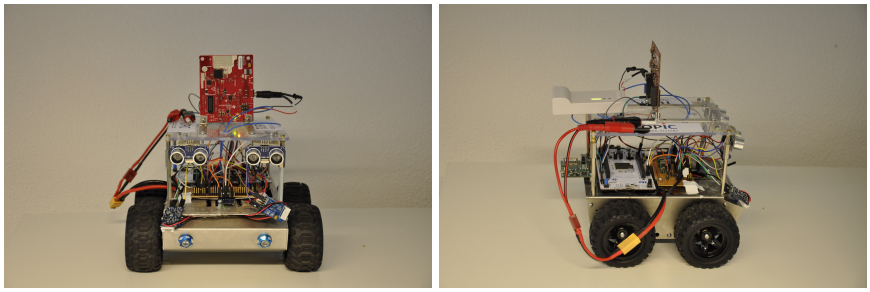

Figure. 3.9: Hind and side views of the designed testbed.

Sensor	**Price (€)**
NUCLEO-L4R5ZI	17.78
DWM1001dev	21.06
MPU6050	4.57
AWR1843BOOST	255
Ultrasound	3.35
Battery 2S Lipo	45.45
Total	347.21

Table 3.1: AGD development cost.

As a note, it is worth mentioning that the Covid-19 situation introduced some major hurdles in this project. Access to the TOPICs office was prohibited for a few months. To continue with the thesis, the option of using a simulation of the vehicle and the environments was discussed. During the lockdown, a substantial amount of time was spent learning how to create virtual environments and 3D modeling on Unity. In Figures 3.10a and 3.10b is shown the simulated environment and the 3D modeling of the vehicle. The lockdown lasted for a few months, so the virtual environment's option was not continued.

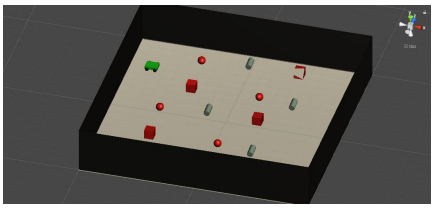

(a) Virtual environment.

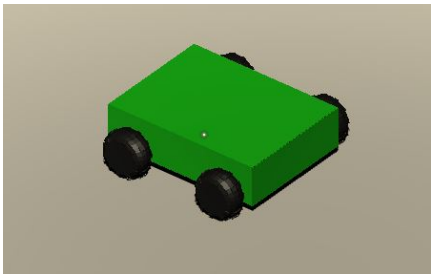

(b) 3D modeling of the AGD.

Figure. 3.10: Unity Virtual TestBed.

Chapter 4

Sensor Fusion: Theory

In previous chapters, it was mentioned that to improve the localization accuracy, a combination of different sensors and fusing their measurements is a common technique. In this chapter we will explain the design and implementation of the fusion of the Radar, IMU, and UWB. In Chapter 3, we described some computations to the raw data of the sensor to get in on the desired units. The data delivered to the fusion algorithm will be:

- Acceleration and orientation of AGD in 2D space computed with the IMU data.
- Position in x and y and V_x and V_y of the AGD computed with UWB data.
- Position in x and y and V_x and V_y of the AGD computed with Radar data.

One of the most common fusion algorithms for localization is the Kalman Filter or variants of it [2, 4, 18, 39, 51]. The sensors used in this thesis are nonlinear; therefore, a simple KF will not be enough. Variations of the KF, such as EKF, AKF, and UKF, will perform efficiently and overcome the nonlinearities. However, AKF and UKF introduce additional computational complexity. If the system were highly nonlinear, techniques such as PF, AKF, or UKF would perform well. In our work, we will employ EKF because of low system nonlinearity as well as to minimize computational complexities and maximize the accuracy associated with the sensor fusion technique.

4.1 EKF Algorithm

Once all the sensors were connected to the MCU, implementing the EKF was the next step. As mentioned before, an EKF is a variation of the Kalman filters that can make accurate nonlinear systems predictions. Kalman filter works as a recursive estimator of the states of a system [34]. This estimation is performed by having some belief of the real state and then applying a correction based on environment's measurements. To overcome the nonlinearities, the EKF performs a linearization of the system. This linearization is made on the system state model and in the measurement model by applying the Jacobians F and H as shown in Equations (4.1) and (4.2). Let S be a matrix of four rows and a single column

containing the system's states, where the states are the position and the speed of the vehicle, f is the system equation to predict the next state, and h is the measurement equations.

$$F = \frac{\delta f}{\delta S} \tag{4.1}$$

$$H = \frac{\delta h}{\delta S} \tag{4.2}$$

In theory, this will be sufficient to estimate the system's states; nevertheless, the measurements are noisy in real scenarios. Therefore the noise has to be taken into consideration in both the system states and measurement model.

4.1.1 System State and Measurements model

The main objective of this work is to get accurate localization of the AGD; therefore, the states to estimate x, y, V_x and V_y. To get the measurement and state-space models are different for every vehicle system. These models have to be designed according to the sensors used; in this case, it was defined that the IMU will be the input sensor for the system state model, and the UWB and Radar will be the measurement sensors for the measurement model. As described in Chapter 3, the IMU will get the acceleration and orientation of the vehicle. By integrating with respect to time the acceleration data, the estimate of the position and the velocity of the AGD can be calculated. As can be seen in Equation (4.3), the states will be predicted with simple physics equations [9]. Here u is the input of the system, A_x and A_y are the acceleration in x and y-axis, respectively, Δt is the time elapsed since the last measurement of the IMU, θ is the orientation angle of the vehicle, and w the noise of the IMU. By applying the Equation (4.1) to the states model S it can be obtained the Jacobian F shown in Equation (4.4)

$$S = f(S,u) = \begin{bmatrix} x \\ y \\ V_x \\ V_y \end{bmatrix} = \begin{bmatrix} x_{(k-1)} + V_x\Delta t + \frac{1}{2}A_x\Delta t^2 \\ y_{(k-1)} + V_y\Delta t + \frac{1}{2}A_x\Delta t^2 \\ V_{x(k-1)} + A_x\Delta t sin\theta \\ V_{y(k-1)} + A_x\Delta t cos\theta \end{bmatrix} + w \tag{4.3}$$

$$F = \begin{bmatrix} 1 & 0 & \Delta t & 0 \\ 0 & 1 & 0 & \Delta t \\ 0 & 0 & 1 & 0 \\ 0 & 0 & 0 & 1 \end{bmatrix} \tag{4.4}$$

The noise will be modeled as white Gaussian noise with a mean of 0 and covariance matrix Q, $w \sim N(0, Q)$. Q will be a diagonal matrix of four rows and four columns with the diagonal values being the variance of the input data, as shown in Equation (4.5) where the σ^2 are the variances of the input variables.

$$Q = \begin{bmatrix} \sigma^2_{A_x} & 0 & 0 & 0 \\ 0 & \sigma^2_{A_y} & 0 & 0 \\ 0 & 0 & \sigma^2_{sin(\theta)} & 0 \\ 0 & 0 & 0 & \sigma^2_{cos(\theta)} \end{bmatrix} \tag{4.5}$$

The variance of each input was determined by reading the IMU data and calculated after 10000 samples. These samples were taken at static position, to determine the noise of the sensors without vehicle movement. The values of the variance for matrix Q were obtained from the IMU are:

$$\begin{aligned} \sigma^2_{A_x} &= 0.00231 \\ \sigma^2_{A_y} &= 0.00060 \\ \sigma^2_{sin(\theta)} &= 0.0003262 \\ \sigma^2_{cos(\theta)} &= 0.0006524 \end{aligned}$$

As the state-space model, the measurement model has been designed with data from the sensors, in this case, the UWB and the Radar. In most sensor fusion cases, there are only two sensors to fuse with the EKF, and the measurement model is the same value as the sensor data. In this case, there are three sensors involved; therefore, the measurement model has to be modified. To take into the equation, the two remaining sensors, we assigned some weight ω to each measurement. This ω denotes how much the values of the measurements be trusted and can take values in the range $[0, 1]$. Let us denote with the subindex u, and r the data from UWB and Radar, respectively, and the noise of the measurements as v. Following Equation (4.2) and applying it to the measurements model, the Jacobian H will be shown in Equation (4.7).

$$Z = h(S) = \begin{bmatrix} x \\ y \\ V_x \\ V_y \end{bmatrix} = \begin{bmatrix} x_u * \omega_{u_x} + x_r * \omega_{r_x} \\ y_u * \omega_{u_y} + y_r * \omega_{r_y} \\ V_{x_u} * \omega_{u_{Vx}} + V_{x_r} * \omega_{r_{Vx}} \\ V_{y_u} * \omega_{u_{Vy}} + V_{y_r} * \omega_{r_{Vy}} \end{bmatrix} + v \tag{4.6}$$

$$H = \begin{bmatrix} \omega_{u_x} + \omega_{r_x} & 0 & 0 & 0 \\ 0 & \omega_{u_y} + \omega_{r_y} & 0 & 0 \\ 0 & 0 & \omega_{u_{Vx}} + \omega_{r_{Vx}} & 0 \\ 0 & 0 & 0 & \omega_{u_{Vy}} + \omega_{r_{Vy}} \end{bmatrix} \tag{4.7}$$

The noise v is a gaussian white noise with mean 0 and covariance matrix R, $v \sim N(0, R)$. R is a diagonal matrix of four rows and four columns with the values of the diagonal being the variance of the measurements data as it can be seen at Equation (4.8) where σ^2_{Zx} is the sum of the product between the variance and the weight of the x component of each the Radar and the UWB (ω_{u_x} * $\sigma^2_{u_x}$ + ω_{r_x} * $\sigma^2_{r_x}$). Also σ^2_{Zy} is the sum of the product between the variance and the weight of the y component of both sensors (ω_{u_y} * $\sigma^2_{u_y}$ + ω_{r_y} * $\sigma^2_{r_y}$). The value of $\sigma^2_{Z_{Vx}}$ is the variance of the speed in x of the UWB ($\sigma^2_{u_{Vx}}$) and $\sigma^2_{Z_{Vy}}$ is the value of

the variance of the speed in y of the UWB ($\sigma^2_{u_{Vy}}$).

$$R = \begin{bmatrix} \sigma^2_{Zx} & 0 & 0 & 0 \\ 0 & \sigma^2_{Zy} & 0 & 0 \\ 0 & 0 & \sigma^2_{ZVx} & 0 \\ 0 & 0 & 0 & \sigma^2_{ZVy} \end{bmatrix} \tag{4.8}$$

All the variances were calculated with the values obtained of 1000 samples from the UWB and the Radar. As in the matrix Q the variances were calculated at static position. The difference is that every 100 samples the position and orientation of the vehicle was changed to consider many scenarios. The weights were obtained based on observation, during the first test it was observed that the results were not as good as expected, even though the accuracy was better than each single sensor. This was because the weights assigned to each sensor were same. Tuning the weights of each sensor was a challenging task, some scenarios yield better performance to a different sensor. By doing several experiments the tuning of the weights was defined. The values obtained are as follows:

- $\sigma^2_{Z_x} = \omega_{u_x} * \sigma^2_{u_x} + \omega_{r_x} * \sigma^2_{r_x} = 0.7 * 0.0846 + 0.3 * 0.2670$
- $\sigma^2_{Z_y} = \omega_{u_y} * \sigma^2_{u_y} + \omega_{r_y} * \sigma^2_{r_y} = 0.7 * 0.0454 + 0.3 * 0.1165$
- $\sigma^2_{Z_{Vx}} = \omega_{u_{vx}} * \sigma^2_{u_{Vx}} + \omega_{r_{Vx}} * \sigma^2_{r_{Vx}} = 0.4 * 0.2911 + 0.6 * 0.0291$
- $\sigma^2_{Z_{Vy}} = \omega_{u_{vy}} * \sigma^2_{u_{Vy}} + \omega_{r_{Vy}} * \sigma^2_{r_{Vy}} = 0.4 * 0.2325 + 0.6 * 0.0263$

Once both models are defined, the next step is to define the initial values of the states X and the uncertainty P. The EKF is a recursive algorithm that consists of two main steps, a prediction, and an update.

4.1.2 Prediction

During the prediction phase, the EKF will "predict" the states' following values and the uncertainty. The IMU will be the sensor used in this step of the fusion. The prediction of X is performed using Equation (4.3), based on the previous values and the input data, as can be seen in Equation (4.9). With X_k^-, being the prediction of the states at the time step k.

$$X_k^- = f(X_{k-1}, u_k) \tag{4.9}$$

The prediction of the uncertainty will be calculated using the Jacobian in Equation (4.1), the previous uncertainty, and the covariance matrix Q in Equation (4.5) to take into account the errors of the IMU. P_k^- is the prediction of the uncertainty at the time step k.

$$P_k^- = FP_{k-1}F^T + Q \tag{4.10}$$

During the first prediction, the EKF will use the initial values as the X_{k-1} to calculate the next step. If the initial values are wrong, the EKF will correct the

states in few time steps due to the system's small nonlinearities; if the system were highly nonlinear, there would be a risk of being stuck in a local minimum with wrong initial values.

4.1.3 Update

The update of EKF is a correction to the prediction using the data from the measurements. These measurements will be the x, y, V_x, and V_y coming from the Radar and the UWB. As explained before, both sensors' data will have a weight according to the level of trust of each sensor. The update phase start with calculating the innovation covariance matrix (L) [9]. This innovation covariance will be calculated with the Jacobian H, the prediction of the uncertainty P_k^-, and the noise covariance R as it is shown in the following equation.

$$L_k = HP_k^- H^T + R \tag{4.11}$$

The computation of S will be used to calculate the Kalman gain (K), L will be a square matrix of 4X4 dimension. The Kalman gain will be calculated as shown in Equation (4.12), where the transpose of H and the inverse of S are used. Before updating the states, a previous calculation has to be done, that will be the difference between the measurements at time step k and the nominal calculation of the measurements [34]. This difference will be denoted as Z_k^+, as can be seen in the Equation (4.13), the nominal value will be the prediction of the states previously calculated. Therefore Z_k^+ will be the error between the measurements and the prediction.

$$K_k = P_k^- H^T L^{-1} \tag{4.12}$$

$$Z_k^+ = Z_k - h(X_k^-) \tag{4.13}$$

The final step of the EKF is to get the update of the states and the uncertainty. The update of the states is performed following Equation (4.14). This update considers the prediction previously calculated in Section 4.1.2, the error of the measurements, and a Kalman gain. Finally, updating the uncertainty is computed using Equation (4.15). Here I is an identity matrix of 4X4, these values will close the loop of the EKF and then be used to calculate the prediction of the next time step.

$$X_k = X_k^- + K_k Z_k^+ \tag{4.14}$$

$$P_k = (I - K_k H) P_k^- \tag{4.15}$$

Chapter 5

Performance Evaluation

This chapter will discuss the extensive performance evaluation of our testbed and describe the first step towards designing an adaptive strategy for energy-efficient localization without trading-off the accuracy. The performance of our localization technique will be compared with state of the art for localization in indoor environments. The tests were aimed to obtain the localization accuracy, robustness, and power consumption of the system and the end-to-end latency.

5.1 Test Setup

The experiments were performed in three different indoor environments to investigate the performance under diverse physical characteristics of the environments:

- E1: This is a section in an office with a space of $5\,\mathrm{m}$ wide and $6.8\,\mathrm{m}$ long. As in any office, there was some object around and also people moving. The objects are two desks, two chairs, four mid-sized plants on the left side, two mid-sized plants on the top, and a big plant on the center. In Figure 5.1, it can be seen the test environment where the numbers $1, 2, 3$ and 4 in red are where the UWB anchors are located, the arrows X and Y is the positive values of the coordinates on the real map. The origin is the position of the anchor 1. The anchors' position was pre-defined and determined to obtain the best accuracy of UWB. The exact position of the anchors is: 1:(0,0), 2:(3.52,0), 3:(3.65,6.78) and 4:(0.1,6.78).

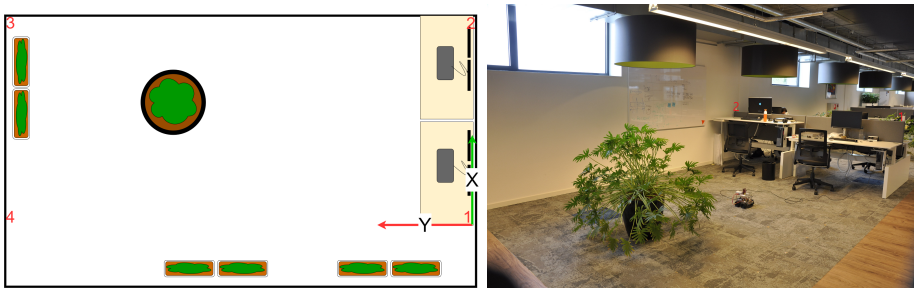

Figure. 5.1: Floor plan and photograph of the test environment E1

- E2: The second environment will be in the same location as E1, with the difference in the density of objects. The purpose of this environment is to observe the performance of the AGD in environments similar to a warehouse, where several objects will be in the path and NLOS scenarios are more probable. This environment can be seen in Figure 5.2.

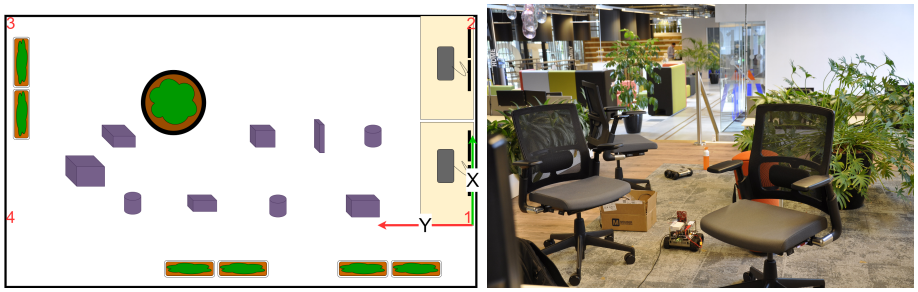

Figure. 5.2: Floor plan and photograph of the test environment E2

- E3: The final environment was in a different place. This was the corridor of a building. The corridor is 14.41 m long and 1.5 m wide. Even though there were no objects in the corridor, the Radar was able to detect the objects inside the apartments. The purpose of this environment is to emulate narrow paths where the vehicle should have accurate localization to prevent crashes. This environment can be seen in Figure 5.3. The position of the UWB anchors is: 1:(-0.75,0), 2:(0.75,0), 3:(0.75,14.41) and 4:(-0.75,14.41).

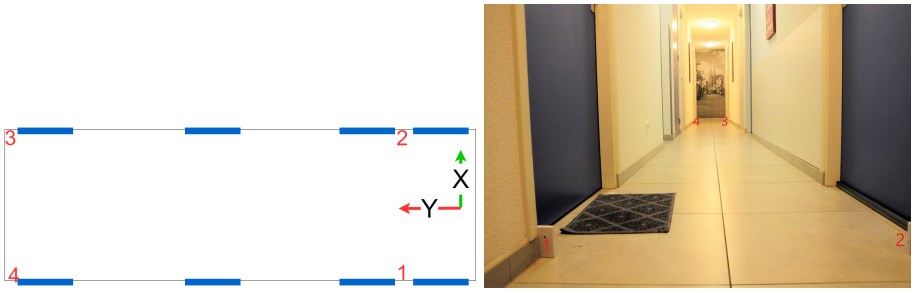

Figure. 5.3: Floor plan and photograph of the test environment E3

5.2 Test Description

The performance evaluation was divided into three parts:

1. Accuracy and Robustness: The performance improvement of our localization method (using UWB, IMU, and Radar) using three sensors over only two of them (the method explored widely in literature). The test will be performed in E1 and E2. The robustness will be tested in E1 and E3, where the vehicle will drive longer paths and more complicated trajectories.

2. Latency: This part will be checked only in E3; note that the localization latency remains robust to the test environment. Therefore performing the test in only one environment is sufficient to obtain complete overview of the performance.

3. Power Consumption: This part will be tested in E3, where the vehicle will perform a continuous drive. The energy will be tested, in different sampling rates, to compare the energy-efficiency of the system and its accuracy.

5.2.1 Accuracy and Robustness

Accuracy

The accuracy was evaluated with three different fusions: Fusion of Radar, UWB and IMU (our method), Fusion of UWB and IMU, and Fusion of Radar and IMU. To evaluate the fusion algorithm's performance, two tests were performed, with initial values of $[x, y, V_x, V_y]$ = [0 m,0 m,0 m/s, 0 m/s]. The initial uncertainty is [0.5 m, 0.5 m, 0 m/s, 0 m/s]. The initial values will not be the exact position in the real world; nevertheless, the system should overcome this error. This test aims to compare the three different fusions and determine which one has better results at low ($1.2\,\mathrm{kmph}$) and high speed ($4\,\mathrm{kmph}$).

To measure accuracy, several test runs have to be made to observe all the vehicle's different behaviors. The accuracy and robustness will be measured in 2 different scenarios at two different speeds, 1.2 and $4\,\mathrm{kmph}$. The first scenario was driving for 4.5 meters straight in E1. To obtain a more accurate measurement, this test was performed with different orientations, in Figure 5.4 can be seen the North and East orientations. The second scenario will be the same as the first one with the variation of using E2 instead. Each scenario was tested twenty times. During the testing will be observed which fusion has the best performance.

Figure. 5.4: Experiments for investigating accuracy of our localization method.

Robustness

The robustness, as the accuracy, consists of two test scenarios. This test was run twenty times at 1.2 kmph and 4 kmph in E1 and E3. The first scenario was also in the office environment with the difference that the vehicle will perform a square trajectory. Finally, the fourth scenario was E3, where the vehicle drive for 13 meters, almost the whole length of the corridor (14 meters). The purpose of this scenario is to observe if there is no accumulation of error. In Figure 5.5 can be seen the second and third scenarios.

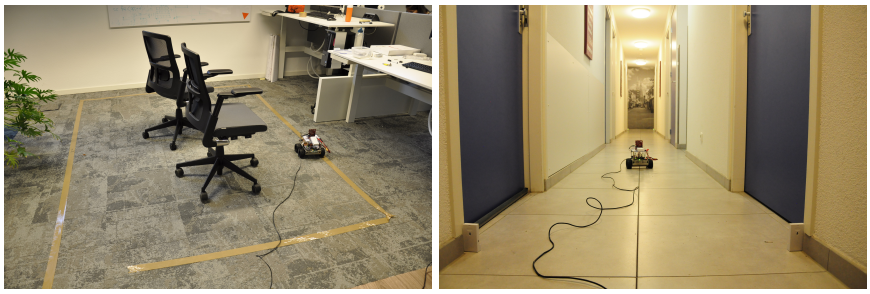

Figure. 5.5: Experiments for investigating robustness of our localization method.

5.2.2 Latency

These tests were in E3, where the vehicle will drive for 13.5 meters at 4 kmph to measure the fusion's latency. A critical factor in autonomous driving is the time to react, therefore having a fast algorithm is essential to perform in real-time. This latency has to consider the time taken to sense the external environment until the localization is achieved. Note that this includes several processes such as sensing, pre-processing, and fusion., as shown in Figure 5.6. The measurements of the latency were only taken in E3.

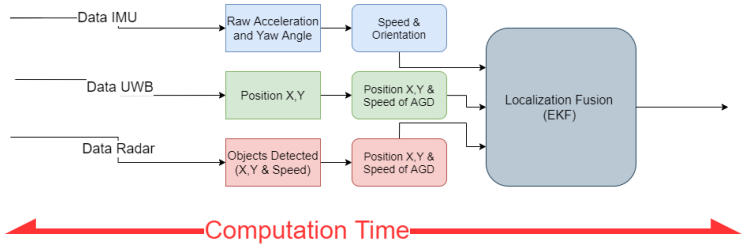

Figure. 5.6: Latency diagram of the system

5.2.3 Power consumption

The fusion with EKF should increase the accuracy of the system; nevertheless, there is an area of opportunity also to reduce the power consumption of it. The task of driving consists of three main actions, drive straight, turn, or brake. The braking action is desired to be minimum to drive as smooth as possible; therefore, the focus will be only on the driving straight action. The EKF will be computed every time a sensor has an update, this meaning that the EKF will have a similar rate as the sensor with the highest sampling rate. In this particular case, the sensor with the highest frequency is the IMU, 1 kHz. While the AGD is driving straight, it is easier to predict the next step. If the difference of orientation measured by the IMU is smaller than one degree per second, the sensors sampling rate can be reduced. Reducing the sampling rate will positively affect power consumption; however, the accuracy will reduce. By performing tests for different sampling rates an optimized behavior of the AGD can be found. The objective is to develop an energy-efficient AGD maximizing the accuracy.

Measuring power consumption was important during this phase. To obtain this measurement, the vehicle battery was charged at its full capacity (8.39 v) and let it discharge with all the systems running, including the motors. Measuring the power consumption of the system was performed with two different approaches. The first one was to calculate with the information from all the sensors and the board's data-sheets. The second approach was performed by making an approximation of the power consumption of each sensor according to its sampling rate. The sampling rates for the whole system varied from 1 Hz to 1 kHz exponentially. These sampling rates will also affect the accuracy of the fusion. Therefore, the localization will be measured during this test for each sampling rate. With this, we compare the trade-off between power consumption and accuracy.

5.3 Results

5.3.1 Accuracy and Robustness

Accuracy

The mean localization error and the standard deviation of the three fusions can be seen in Figure 5.7. In Table 5.1 can be seen as the mean error and the standard deviation of the three fusions fusion methods with AGD driving at low speed. The

Radar and IMU fusion shows the worst behavior in this scenario, and, as expected, the UWB, Radar, and IMU fusion show the best performance. In Table 5.2 are shown the mean error and its standard deviation for the high speed test. The results of the fusions have a Gaussian-like distribution, as can be seen in Figure 5.7. In Figure 5.8, the mean error at low and full speed is shown. All of the fusions show a mean error smaller than 20 cm. Nevertheless, clearly, our method of sensor fusion with the three sensors, UWB, Radar, and IMU, performs better than the fusion of two sensors.

	Mean error (cm)	**Std Dev (cm)**
U,R, & I	9.95	9.51
R, & I	16.57	10.21
U, & I	12.73	8.03

Table 5.1: Mean error and Standard Deviation at 1.2 kmph.

	Mean error (cm)	**Std Dev (cm)**
U,R, & I	8.42	8.71
R, & I	14.60	9.14
U, & I	15.78	10.99

Table 5.2: Mean errror and Standard Deviation at 4 kmph.

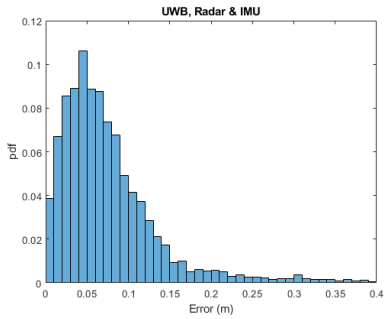

Figure. 5.7: Error distribution fusion of UWB, Radar and IMU.

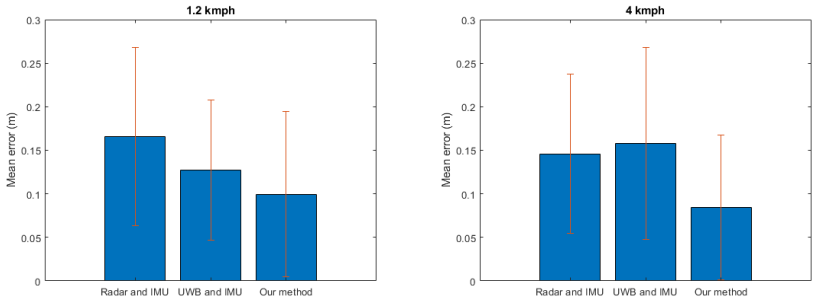

Figure. 5.8: Mean localization error and standard deviation of the different fusions and speed profiles.

In Figure 5.9 we present the absolute error of the three fusions is compared. The error was plotted with the average of all the test runs. As can be observed, our method shows a better prediction than the other methods. The fusions of UWB-Radar-IMU and UWB-IMU show a considerable error at the starting point; this is due to the difference between the initial position and the UWB data. This error is corrected after the AGD runs for a few seconds. In the fusion of Radar and IMU, it shows an increase of the error at the beginning of the run. This increase is a consequence of the initial acceleration of the AGD.

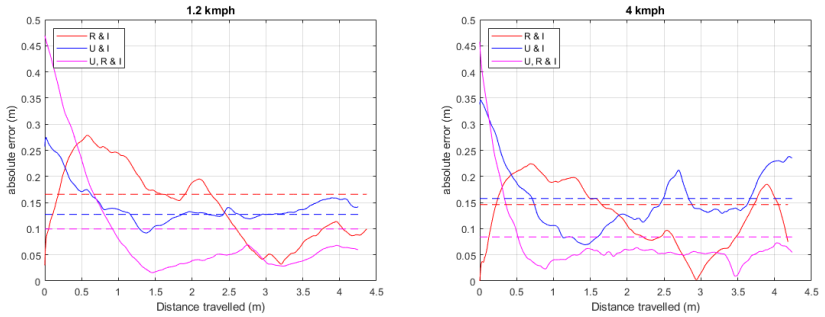

Figure. 5.9: Variation of localization error with respect to euclidean distance between current and initial position.

By analyzing the results, it was determined that the combination of the UWB, Radar, and IMU delivers the best results at both speeds. An interesting aspect is the small improvement of the fusion of Radar & IMU and the UWB, Radar & IMU at 4 km/hr compared to the 1.2 km/hr. This improvement is because the Radar calculates the distance to the objects by considering the Doppler effect; therefore, when the vehicle is static or driving at low speed, the measurements get noisier [50, 7, 48]. In the case of the fusion of the UWB & IMU the error increases while the speed increases due to the sampling frequency of the UWB.

Robustness

The square trajectory test was performed in E1, and the vehicle drives around a pair of chairs. To get a complete evaluation of the AGD performance, 20 test runs were performed. During this test, the vehicle will be tested in all different orientations and perform turns.

Another test performed is with a high density of objects; this was performed in E2. The purpose of the test was to evaluate the behavior of the AGD in environments with a high-density of objects. A total of 20 test runs were performed.

Finally, in E3, the test of driving 13.5 m was evaluated; in this scenario, there will not be any object in the corridor. However, the Radar should be able to detect objects behind the doors. Figure 5.10 shows the mean localization error and standard deviation of the three tests. Table 5.3 shows the mean values obtained of these three tests. The performance of our method is similar to the results obtained

previously.

	E1		E2		E3	
Speed	**Mean error (cm)**	**Std Dev (cm)**	**Mean error (cm)**	**Std Dev (cm)**	**Mean error (cm)**	**Std Dev (cm)**
1.2 kmph	10.48	9.41	9.80	8.25	8.89	5.49
4 kmph	9.38	8.77	8.70	7.26	8.45	6.77

Table 5.3: Mean localization error and standard deviation of E1, E2 and E3.

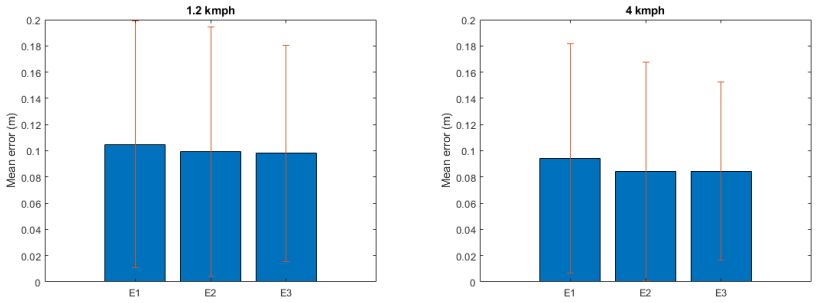

Figure. 5.10: Mean localization error and standard deviation in three different environments and speed profiles.

Figure 5.11 can be observed the real and the predicted vehicle position during these tests. This trajectory was challenging to follow the same route every time. During the square trajectory, it was not possible to get a 100 % accurate real position; therefore, an approximation was performed as seven straight lines. As can be seen, the vehicle turns are where the most significant errors occur; this will be one reason for the small increase of the mean error. Another reason is that the Radar gets an increase in the errors while turning due to this sensor can not measure the changes in the orientation angle.

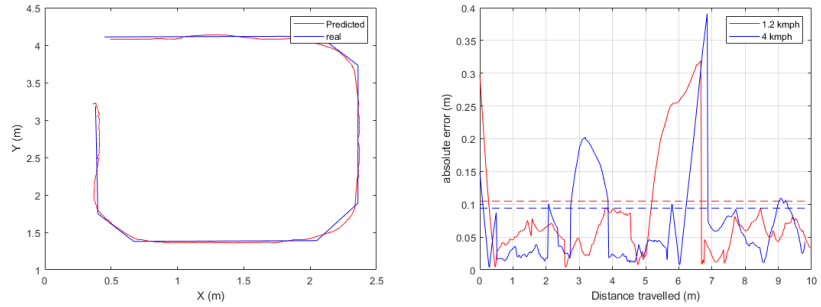

Figure. 5.11: Absolute error as a function of Eucliean distance of the vehicle from initial position in a square trajectory test in E1.

The absolute error of the tests in E2 and E3 can be observed in Figures 5.12 and 5.13 respectively. The systems show robustness against different environments and trajectories of the AGD. Therefore, it can be said that our method is robust.

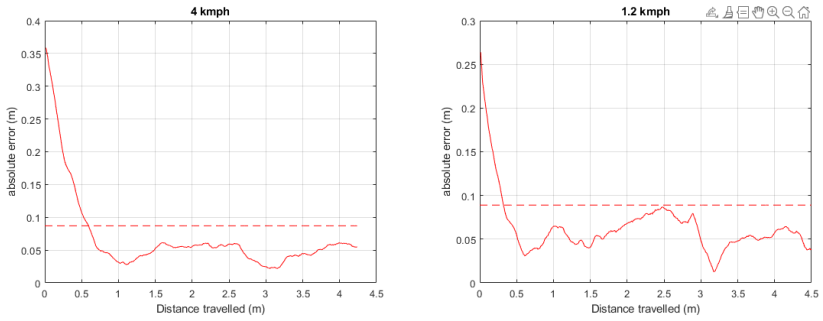

Figure. 5.12: Absolute error as a function of Eucliean distance of the vehicle from initial position in a 4.5 meters trajectory test in E2.

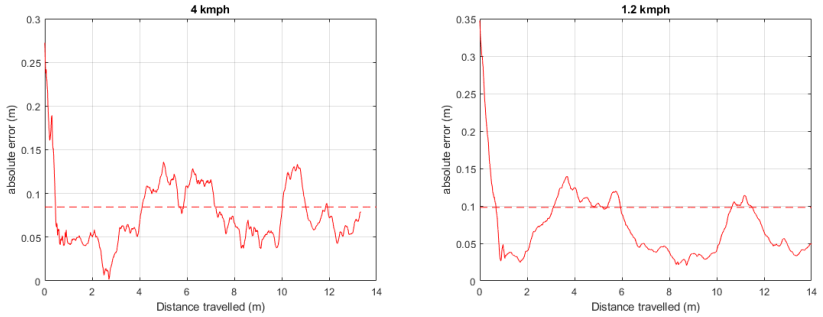

Figure. 5.13: Absolute error as a function of Eucliean distance of the vehicle from initial position in a 13.5 meters trajectory test in E3.

5.3.2 Latency

The latency measurements were taken while the vehicle moved around to have a better estimation of when the data is changing. To calculate the latency of the algorithm, 120,000 samples were used as data. The latency obtained shows Gaussian distribution, as shown in Figure 5.14. The mean and the standard deviation of the latency are 3.218 ms and 0.533 ms respectively. Our results show a latency sufficient to perform in real-time. The measurement of the latency is considered accurate for all the environments.

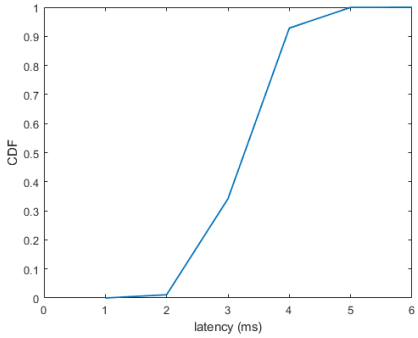

Figure. 5.14: CDF of localization latency of our system

5.3.3 Power Consumption

Besides the latency of the system, another significant factor in industry is power consumption. In the AGD used, the elements that are powered by the battery are shown in Figure 3.10.a. To measure the power consumption of the motors while moving was not possible in this analysis. Therefore the analysis will only be performed on the sensors and the board. The power consumption obtained from the data-sheet can be seen in the table below.

	Average (W)	**Maximum (W)**
NUCLEO-L4R5ZI	1.5	1.575
DWM1001dev	0.67	0.737
MPU6050	0.01289	0.01418
AWR1843BOOST	1.92	2.67
Total	4.1029	4.9918

Table 5.4: Power consumption of the system [50, 45, 11, 21]

The power consumption obtained during the tests is shown in Figure 5.15, where power consumption and mean localization error are plotted as functions of sampling rate in logarithmic scale. It can be seen that while the mean error is a decreasing function of sampling rate, the power consumption is an increasing function of it. Interestingly, it can also be noticed that beyond 32 Hz, there is only a marginal improvement in the localization accuracy. On the other hand, power consumption increases linearly with the sampling rate. This suggests that there is a huge potential for making our system extremely energy-efficient without trading off the localization accuracy by tuning the sampling rate of the sensors.

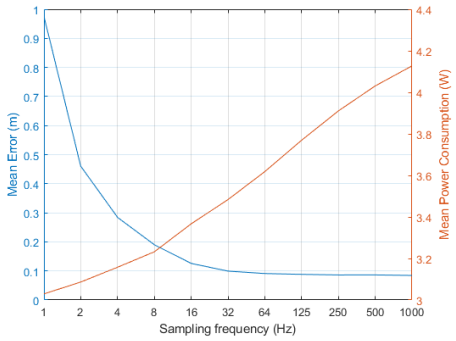

Figure. 5.15: Power consumption vs Sampling rate vs Mean error

5.4 Comparison against state of the art

The results obtained during this thesis will be compared against four different fusions for indoor environment. It will be compared the speed, accuracy, deviation, latency, and operating frequency to make an accurate analysis. The four different fusions to compare the results of this thesis are:

1. Radar and ultrasound [56]
2. UWB and IMU [2]
3. LiDAR and UWB [55]
4. LiDAR, UWB, and IMU [53]

In our proposed AGD, the trade off between speed and accuracy shows better results. The systems' latency is smaller than the 3 ms of the fusion of LiDAR and UWB [55]. A considerable advantage of our methodology is the development cost; three of them exceed the $ 4000 . It is important to note that $ 4500 is only the cost of the LiDAR and the $ 4000 the cost of the mobile robot.

	Radar & US	**UWB & IMU**	**LiDAR & UWB**	**UWB, LiDAR & IMU**	**UWB, Radar & IMU**
Speed (km/hr)	4.32	2.5	2.88	2.52	4
Accuracy (cm)	15	10.2	7.6	10	8.54
Std Dev (cm)	10.24	–	12.2	–	7.39
Latency (ms)	–	–	3	–	2.66
Cost	4000 (USD)**	–	4,500.00 (USD)*	4,500.00 (USD)*	347.21 (€)
Power Consumption (W)		–	8*	8*	4.1029

Table 5.5: Fusion for indoor localization.
∗Lidar value. ∗∗ Mobile robot cost

The comparison of the power consumption of the system will be performed only with the Radar. The sensor with the highest consumption will be compared against LiDARs used in [38, 53, 14]. In Table 5.6 it can be seen that the Radar has a lower consumption than the LiDARs.

	Velodyne HDL64E	**Velodyne VLP-16**	**Hokuyo UTM-30LX-EW**	**Hokuyo UST-05LN**	**AWR1843BOOST**
Average Consumption (W)	60	8	8	3.6	1.77
Max Consumption (W)	60	8	8	9.6	2.14

Table 5.6: Power Consumption Radar VS LiDAR.

As can be observed from Tables 5.5 and 5.6, the accuracy obtained with the fusion of UWB, Radar, and IMU is similar to the accuracy of state of the art. The advantage of this design is that the computation time is reduced compared and also power consumption.

Chapter 6

Conclusions and Future Work

With autonomous vehicles gaining an ever-increasing attention of academia and industries, it is crucial to localize them with accuracies in the scale of a few centimeters in an energy-efficient manner. In this thesis, we addressed this challenge of localization for autonomous vehicles in indoor environments where standard localization techniques using GPS cease to work. Our contributions in this thesis are manifold.

- We developed a low-cost, energy-efficient Autonomous Ground Drone (AGD) equipped with UWB, IMU, and Radar for the purpose of localization.
- We employed EKF to combine the signals acquired by these sensors in order to enable reliable localization. We demonstrated that our localization method can achieve a mean accuracy of 8 cms in a variety of test environments. Further, the localization can be performed in real-time with a mean latency of 3 ms. Our method outperforms state of the art in localization.
- We investigated the accuracy and energy-efficiency of our system as a function of sensing sampling rate and demonstrated that the energy consumption can be reduced substantially without trading off the localization accuracy.

6.1 Future Work

Despite the promising results obtained by this research, few upgrades can be done to the system to increase accuracy. As noted in Chapter 3, the Radar work with a limited FOV of $\pm 100^{\circ}$, and as it was explained in the results, the Radar is sensitive to low-speed objects. Nevertheless, some work has been done with beam steering techniques to overcome the sensitivity and increase the FOV [8, 36]. This upgrade will probably reduce the noise, increase the Radar's detection, and, in consequence, the accuracy of the EKF.

The sensors selected have the desired behavior for localization on autonomous driving, but some capabilities have not been explored in this thesis, such as communi-

cation of the UWB. With these set of sensors can be performed: Object detection, tracking objects, and path planning. Besides, applying the beam steering to the Radar to increase the system's performance will be difficult with just one vehicle. Therefore explore the performance of a network of AGDs is a future step in the evolution of this project.

While analyzing the results, we notice that there is an opportunity to develop an adaptation to the EKF to increase the accuracy in turns and also reduce the power consumption by modifying, in real-time, the sampling rate of the sensors.

Bibliography

[1] A. Sabanovíc A. J. van Katwijk and P. P. Verton. Person detection using ultra-wideband radars uwb indoor person tracking. Master's thesis, Delft University of Technology, Delft, The Netherlands, 2017.

[2] Alvin Marquez, Brinda Tank, Sunil Kumar Meghani, Sabbir Ahmed and Kemal Tepe . Accurate UWB and IMU based Indoor Localization for Autonomous Robots . *IEEE 30th Canadian Conference on Electrical and Computer Engineering (CCECE)*, (30), June 2017.

[3] Andreas Biri, Neal Jackson, Lothar Thiele, Pat Pannuto and Prabal Dutta. SociTrack: Infrastructure-Free Interaction Tracking through Mobile Sensor Networks. *26th Annual International Conference on Mobile Computing and Networking (MobiCom)*, 2020.

[4] Ashraf Abosekeen,Aboelmagd Noureldin and Michael J. Korenberg. Terrain-based Vehicle Localization Using Low Cost MEMS-IMU Sensors. *2016 IEEE 83rd Vehicular Technology Conference (VTC Spring)*, 2016.

[5] Ashraf Abosekeen,Aboelmagd Noureldin and Michael J. Korenberg. Utilizing the ACC-FMCW Radar for Land Vehicles Navigation. *2018 IEEE/ION Position, Location and Navigation Symposium (PLANS)*, 23(26), 2018.

[6] B. Ramirez, H. Chung3, H. Derhamy, J. Eliasson, and J.C. Barca. Relative localization with Computer Vision and UWB Range for Flying Robot Formation Control. *14th International Conference on Control, Automation, Robotics Vision (ICARCV)*, 13(15), November 2016.

[7] Cesar Iovescu,Sandeep Rao, Texas Instruments. The fundamentals of millimeter wave sensors. 2017.

[8] Clemens Pfeffer, Reinhard Feger, Christoph Wagner and Andreas Stelzer. FMCW MIMO Radar System for Frequency-Division Multiple TX-Beamforming. *IEEE Transactions on Microwave Theory and Techniques*, 2013.

[9] Damien Veillard, Frederick Mailly and Philippe Fraisse. EKF-based State Estimation for Train Localization. *IEEE Sensor*, 2017.

[10] Decawave. Product Overview. 2017.

[11] Decawave. Product Datasheet: DWM1001-DEV. 2017.

[12] Decawave. DWM1001 Firmware User Guide Based on DWM1001-DEV board. 2017.

[13] Elec Freaks. Ultrasonic Ranging Module HC - SR04. 2017.

[14] Xinyu Gao. Sensor data fusion of lidar and camera for road user detection. Master's thesis, Delft University of Technology, Delft, The Netherlands, 2018.

[15] Gia-Minh Hoang1, Benoit Denis, Jérome Härri and Dirk T.M. Slock . Robust Data Fusion for Cooperative Vehicular Localization in Tunnels. *IEEE Intelligent Vehicles Symposium (IV)*, 11(14), June 2017.

[16] Goran Vasiljevic, Frano Petric and Zdenko Kovacic. Multi-layer Mapping-based Autonomous Forklift Localization in an Industrial Environment. *22nd Mediterranean Conference on Control and Automation (MED)*, 2014.

[17] Guillaume Bresson , Zayed Alsayed, Li Yu, and S´ebastien Glaser. Simultaneous Localization and Mapping: A Survey of Current Trends in Autonomous Driving . *IEEE TRANSACTIONS ON INTELLIGENT VEHICLES*, 2(3), September 2017.

[18] Guowei Wan, Xiaolong Yang, Renlan Cai, Hao Li, Yao Zhou, Hao Wang and Shiyu Song. Robust and Precise Vehicle Localization based on Multi-sensor Fusion in Diverse City Scenes. *IEEE International Conference on Robotics and Automation (ICRA)*, 21(25), May 2018.

[19] Haoqian Wang , Member, IEEE, Yi Luo, Wangpeng An , Qingyun Sun, Jun Xu , and Lei Zhang. PID Controller-Based Stochastic Optimization Acceleration for Deep Neural Networks. *IEEE TRANSACTIONS ON NEURAL NETWORKS AND LEARNING SYSTEMS*, 2020.

[20] Instructables. Accelerometer Gyro Tutorial. `https://content.instructables.com/pdfs/E59/IJSB/G4PBOJPB/Accelerometer-Gyro-Tutorial.pdf`, 2010. Last accessed: Jamuary, 2010.

[21] InvenSense Inc. MPU-6000 and MPU-6050 Register Map and Descriptions Revision 4.2. 2013.

[22] Ivana Shopovska, Ljubomir Jovanov, Peter Veelaert, Peter Veelaert, Kris Lehaen, Flanders Make and Wilfried Philips. A Hybrid Fusion Based Frontal-Lateral Collaborative Pedestrian Detection and Tracking. *International Conference on Intelligent Transportation Systems (ITSC)*, (20), 2017.

[23] Joelle Al Hage, Maan E.El Najjar and Denis Pomorski . Fault Tolerant Multi-Sensor Fusion for Multi-Robot Collaborative Localization. *IEEE lntemational Conference on Multisensor Fusion and Integration for Intelligent Systems (MFI)*, 19(21), September 2016.

[24] K. Golestan, F. Sattar∗, F. Karray, M. Kamel and S. Seifzadeh. Localization in vehicular ad hoc networks using data fusion and V2V communication. *The International Journal for the Computer and Telecommunications Industry*, 61 (72), July 2016.

[25] Karl Berntorp , Tru Hoang, and Stefano Di Cairano. Motion Planning of Autonomous Road Vehicles by Particle Filtering . *IEEE TRANSACTIONS ON INTELLIGENT VEHICLES*, 4(2), June 2019.

[26] Kuan-Hui Lee, Yusuke Kanzawa, Matthew Derry, Michael R. James. Multi-Target Track-to-Track Fusion Based on Permutation Matrix Track Association. *Intelligent Vehicles Symposium (IV)*, 26(30), 2018.

[27] Kyeong-Eun Kim, Chang-Joo Lee, Dong-Sung Pae and Myo-Taeg Lim. Sensor Fusion for Vehicle Tracking with Camera and Radar Sensor. *International Conference on Control, Automation and Systems (ICCAS)*, 18(17), October 2017.

[28] Marco Karrer, Mohit Agarwal, Mina Kamel, Roland Siegwart and Margarita Chli. Collaborative 6DoF Relative Pose Estimation for two UAVs with Overlapping Fields of View. *IEEE International Conference on Robotics and Automation (ICRA)*, 21(25), May 2018.

[29] Michael Aeberhard, Stefan Schlichthärle, Nico Kaempchen, and Torsten Bertram. Track-to-Track Fusion With Asynchronous Sensors Using Information Matrix Fusion for Surround Environment Perception. *IEEE TRANSACTIONS ON INTELLIGENT TRANSPORTATION SYSTEMS*, 13(4), December 2012.

[30] Microchip. ATmega640/V-1280/V-1281/V-2560/V-2561/V. 2014.

[31] Milos Vasic, David Mansolino, and Alcherio Martinoli. A System Implementation and Evaluation of a Cooperative Fusion and Tracking Algorithm based on a Gaussian Mixture PHD Filter. *IEEE International Conference on Robotics and Automation (ICRA)*, 21(25), May 2018.

[32] Mohammed A. H. Ali and Musa Mailah. Path Planning and Control of Mobile Robot in Road Environments Using Sensor Fusion and Active Force Control . *IEEE TRANSACTIONS ON VEHICULAR TECHNOLOGY*, 68(3), March 2019.

[33] Moon-Hyung Song, Chang-il Kim, Jong-Min Kim, Kwang-Soo Lee, Hyun-Bae Park, Jae-Seok Jeon, Su-Jin Kwag and Moon-Sik Kim. A Novel Approach to the Enhancement of Lane Estimator by using Kalman Filter. *17th International Conference on Control, Automation and Systems (ICCAS)*, 2017.

[34] Rudy Negenborn. Robot localization and kalman filters on finding your position in a noisy world. Master's thesis, Utrecht University, Utrecht, The Netherlands, 2003.

[35] Jeroen Overman. Wireless clock synchronisation for uwb positioning. Master's thesis, Delft University of Technology, Delft, The Netherlands, 2019.

[36] Pascual Hilario Re, Cristian Alistarh, Symon Podilchak, George Goussetis, John Thompson, Jaesup Lee. Millimeter-Wave FMCW Radar Development using SIW Butler Matrix for Time Domain Beam Steering. *16th European Radar Conference (EuRAD)*, 2019.

[37] Patrick Geneva, Kevin Eckenhoff, and Guoquan Huang. Asynchronous Multi-Sensor Fusion for 3D Mapping and Localization. *IEEE International Conference on Robotics and Automation (ICRA)*, 21(25), May 2018.

[38] Qi Chen, Sihai Tang, Qing Yang and Song Fu. Cooper: Cooperative Perception for Connected Autonomous Vehicles based on 3D Point Clouds. *IEEE 39th International Conference on Distributed Computing Systems (ICDCS)*, (39), May 2019.

[39] Qingxi Zeng, Dehui Liu and Chade Lv. UWB/Binocular VO Fusion Algorithm Based on Adaptive Kalman Filter. *International Sensor Open Access Journal*, 2019.

[40] Roland Hostettler and Petar M. Djuric. Vehicle Tracking Based on Fusion of Magnetometer and Accelerometer Sensor Measurements With Particle Filtering . *IEEE TRANSACTIONS ON VEHICULAR TECHNOLOGY*, 64(11), November 2015.

[41] Roshan Ayyalasomayajula, Aditya Arun†, Chenfeng Wu, Sanatan Sharma, Abhishek Rajkumar Sethi, Deepak Vasisht and Dinesh Bharadia. Deep Learning based Wireless Localization for Indoor Navigation. *26th Annual International Conference on Mobile Computing and Networking (MobiCom)*, 2020.

[42] SAE. SAE International Releases Updated Visual Chart for Its "Levels of Driving Automation" Standard for Self-Driving Vehicles. `https://www.sae.org/news/press-room/2018/12/sae-international-\releases-updated-visual-chart-for-its-"levels-of-driving-\automation"-standard-for-self-driving-vehicles`, 2018. Last accessed: December, 2019.

[43] Sampo Kuutti, Saber Fallah , Konstantinos Katsaros, Mehrdad Dianati, Francis Mccullough, and Alexandros Mouzakitis. A Survey of the State-of-the-Art Localization Techniques and Their Potentials for Autonomous Vehicle Applications. *IEEE INTERNET OF THINGS JOURNAL*, 5(2), April 2018.

[44] Shin, HY., Tsourdos, A., Lappas, V., Ampatzoglou, A., Kostopoulos, V., S. Bertrand, J. Marzat, H. Piet-Lahanier, Lindgren, M. Detratti. Autonomous Unmanned Heterogeneous Vehicles for Persistent Monitoring. *AIAA SciTech Forum*, 2019.

[45] STMicrocontrollers. STM32 Nucleo-144 boards User Manual. 2019.

[46] STMicrocontrollers. STM32L476xx. 2019.

[47] STMicrocontrollers. STM32L4R5xx STM32L4R7xx STM32L4R9xx Datasheet. 2020.

[48] Texas Instruments. AWR18xx/16xx/14xx/68xx Technical Reference Manual. May 2017.

[49] Texas Instruments. Programming Chirp Parameters in TI Radar Devices. May 2017.

[50] Texas Instruments. xWR1843 Evaluation Module (xWR1843BOOST) Single-Chip mmWave Sensing Solution. 2018.

[51] Thien Minh Nguyen, Abdul Hanif Zaini, Kexin Guo and Lihua Xie. An Ultra-Wideband-based Multi-UAV Localization System in GPS-denied environments. *International Micro Air Vehicle Conference and Competition 2016 (IMAV 2016)*, 17(21), 2016.

[52] Tzu-Kuang Lee, Yu-Chiao Kuo, Shih-Hsuan Huang, Guan-Sheng Wang, Chih-Yu Lin and Yu-Chee Tseng . Augmenting Car Surrounding Information by Inter-Vehicle Data Fusion. *IEEE Wireless Communications and Networking Conference (WCNC)*, 2019.

[53] Weikun Zhen and Sebastian Scherer. Estimating the Localizability in Tunnel-like Environments using LiDAR and UWB. *International Conference on Robotics and Automation (ICRA)*, 20(24), May 2019.

[54] Xu Li, Ching-Yao Chan, and Yu Wang. A Reliable Fusion Methodology for Simultaneous Estimation of Vehicle Sideslip and Yaw Angles . *IEEE TRANSACTIONS ON VEHICULAR TECHNOLOGY*, 65(6), June 2016.

[55] Yang Song, Mingyang Guan, Wee Peng Tay, Choi Look Law and Changyun Wen. UWB/LiDAR Fusion For Cooperative Range-Only SLAM. *International Conference on Robotics and Automation (ICRA)*, 20(24), May 2019.

[56] Yassen Dobrev, Sergio Flores and Martin Vossiek. Multi-Modal Sensor Fusion for Indoor Mobile Robot Pose Estimation. *IEEE/ION Position, Location and Navigation Symposium (PLANS)*, 11(14), May 2016.

[57] Mohammadreza Yavari. Indoor real-time positioning using ultra-wideband technology. Master's thesis, University of New Brunswick Fredericton, New Brunswick, Canada, 2015.